JPRS 75565
25 April 1980

China Report

SCIENCE AND TECHNOLOGY

No. 34

FBIS FOREIGN BROADCAST INFORMATION SERVICE

NOTE

JPRS publications contain information primarily from foreign newspapers, periodicals and books, but also from news agency transmissions and broadcasts. Materials from foreign-language sources are translated; those from English-language sources are transcribed or reprinted, with the original phrasing and other characteristics retained.

Headlines, editorial reports, and material enclosed in brackets [] are supplied by JPRS. Processing indicators such as [Text] or [Excerpt] in the first line of each item, or following the last line of a brief, indicate how the original information was processed. Where no processing indicator is given, the information was summarized or extracted.

Unfamiliar names rendered phonetically or transliterated are enclosed in parentheses. Words or names preceded by a question mark and enclosed in parentheses were not clear in the original but have been supplied as appropriate in context. Other unattributed parenthetical notes within the body of an item originate with the source. Times within items are as given by source.

The contents of this publication in no way represent the policies, views or attitudes of the U.S. Government.

PROCUREMENT OF PUBLICATIONS

JPRS publications may be ordered from the National Technical Information Service, Springfield, Virginia 22161. In ordering, it is recommended that the JPRS number, title, date and author, if applicable, of publication be cited.

Current JPRS publications are announced in Government Reports Announcements issued semi-monthly by the National Technical Information Service, and are listed in the Monthly Catalog of U.S. Government Publications issued by the Superintendent of Documents, U.S. Government Printing Office, Washington, D.C. 20402.

Indexes to this report (by keyword, author, personal names, title and series) are available from Bell & Howell, Old Mansfield Road, Wooster, Ohio 44691.

Correspondence pertaining to matters other than procurement may be addressed to Joint Publications Research Service, 1000 North Glebe Road, Arlington, Virginia 22201.

JPRS 75565

25 April 1980

CHINA REPORT

SCIENCE AND TECHNOLOGY

No. 34

CONTENTS

ABSTRACTS

CONTENTS (Continued)

PHYSICAL SCIENCES

SOUTH CHINA SEA RESOURCES CALLED EXPANSIVE

Beijing DILI ZHISHI [GEOGRAPHICAL KNOWLEDGE] in Chinese No 6, Jun 79 pp 5-6, 11

[Article by Li Jiansheng [2621 1696 3932] and Chen Shijian [7115 0670 1017]: "The Expansive South Sea"]

[Text] The expansive South Sea (also called the South China Sea) with its green waves covering tens of thousands of hectares is the southern frontier of the motherland and also our nation's southernmost and the largest ocean region covering an area of 3.6 million square kilometers, three times as large as the total area of Bohai, Huanghai and Donghai.

The South Sea is surrounded by the Asian continent, the Philippine Islands and Kalimantan Island. To the north lie Guangxi and Guangdong provinces of the continent, to the west lies the Indochina-Malaysia Peninsula, to the east are the Philippine Islands, to the south lies the northern edge of Asia's largest island--Kalimantan Island (also called Borneo). The eastern border of the South Sea extends from the ridge zone of the Penghu Islands of the Taiwan Straits to the northeast of the South Sea (separated from Donghai by the line extending from Oluanpi at the southern tip of Taiwan and along the shallow beaches of Taiwan to the border of Fujian and Guangdong. The South Sea also connects with the Bashi Channel and the Philippine Sea and the Pacific. At the southwest it connects with the Malacca Strait and the Andaman Sea and the Indian Ocean. The east connects with the Mindoro Strait, the Balabac Strait and the Sulu Sea. The average depth of the South Sea is greater than 1,000 meters and the deepest part is 5,567 meters. At the center is a deep sea ocean basin. Its north and southwest parts are surrounded by continental shelf (the natural extension of land at the sea bottom) and continental slope (the slope of the continental shelf that extends to 3,000 to 4,000 meters at the bottom of the sea). The southeast part and the eastern part belong to the underwater island and continental slope regions. The entire sea is shaped like a rhombus extending from the northeast to the southwest.

On the surface of this expansive South Sea are scattered clusters of coral reefs, shallow beaches and hidden shoals. The background of clean white

coral reef basins of the sky blue sea water shines like a string of pearls scattered on a giant plate of green jade. These "shining pearls of the sea" of our motherland are the islands of the South Sea--the Tungsha Archipelago, the Zhongsha Archipelago and the Nansha Archipelago. The James shoal Islands are our nation's southernmost frontier.

The geographical positions of the islands of the South Sea are very important. They are at the neck of traffic between the Pacific and the Indian Oceans. They are the relay stations of traffic from Asia to the Oceania. They are on the essential routes of seagoing traffic between Asia and Southeast Asian nations and the African and European continents.

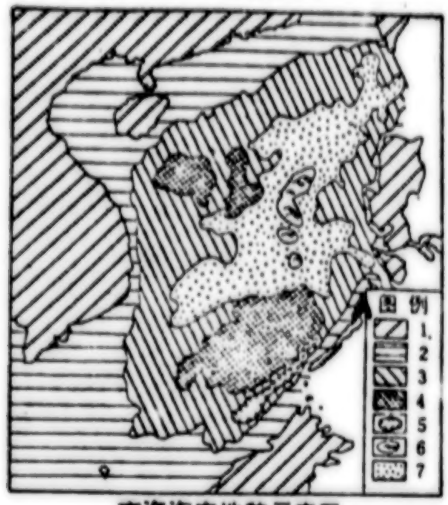

南海海底地貌示意图

Illustrative Map of the landform at the bottom of the South Sea

KEY:
1. Land
2. Continental shelf
3. Continental slope
4. Xisha-Zhongsha plateaus of the sea floor
5. Ocean trench
6. Oceanic mountain
7. Deep sea plains

A. Legend

The Magnificent Sight of the Landforms of the Bottom of the Sea

The landforms of the ocean regions of the South Sea are extremely complex, from the continental shelf to the deep sea plains and plateaus at the bottom of the sea, from coral reefs to landforms formed by the eruption of volcanos,

from islands that rise up from the surface of the sea to underwater valleys several thousand meters below the surface of the sea. They are of all kinds and are magnificent to view.

The South Sea is one of a series of sea basins along the eastern edge of the Asian continent. It is a sea at the edge of the continent. It is surrounded by extensive continental shelf formations. Near the mouth of the Zhujiang (Pearl River) is a continental shelf of an average width of 233 kilometers. The average width of the continental shelf of the Guangzhou Gulf is 292 kilometers. The average width of the continental shelf of the southeast region of Hainan Island is 114 kilometers. The Northern Gulf is a closed continental shelf similar to that of Bohai. The material composition of the continental shelf of this region indicates the material mainly comes from rivers of the coastal regions of Guangdong. The original rock was a kind of igneous rock formed by the Yanshan tectonic movement during the Mesozoic--granite. It contains a rich content of quartz and potash feldspar and large amounts of microorganisms. The entire area of the continental shelf covers 800,000 square kilometers.

In the southwest region of the South Sea, i.e., the Indochina Peninsula, Malaysian Peninsula, the Sumatra Islands and Kalimantan Island, the vast expanse of the continental shelf among these islands drops into the deep sea plain like a ladder. The widest place is in the Gulf of Siam with a width of over 500 kilometers and an average depth of 40 meters of sea. The southeastern region of the South Sea and its eastern continental shelf are generally narrower. On the west side of Luzon Island the width is only 18 kilometers.

The second is the deep sea plains which lie at 3,500 to 4,500 meters below the surface as flat sea floors or hilly plains. On the plains are often found high rising mountain ranges over 3,000 meters high, mostly formed by volcanic eruptions at the bottom of the sea. Besides the mountain ranges on the plains at the bottom of the sea there are also depressed basins. At the central part of the deep sea plain of the South Sea are three such narrow and long basins at a depth of over 5,000 meters. The major materials that make up the deep sea plains include globigerina ooze as well as volcanic ash.

Plateaus at the bottom of the sea rise up from the sea floor but generally not beyond the surface of the sea. The plateuas are not large in scale and are shaped like irregular rotundas. For example, the top of the plateaus of the deep sea plateaus of Xisha and Nansha are all over 1,000 meters below the surface of the sea and the average depth of the top of the plateaus of the deep sea plateaus of Nansha are about 1,700 meters. On top of the plateaus are ideal localities for parasitic existence of coral polyp. Therefore coral reefs are very developed. When the coral reefs gradually rise above the surface of the sea along with the upward movement of the crust, they form coral islands. Only the pointed rocks in the Xisha archipelago are small islands formed from volcanic breccia.

Over 10 underwater volcanic peaks have been found among the Zhongsha Archipelago and the Xisha Archipelago. Among these coral islands, hidden coral reefs and shoals is a huge underwater valley dropping to a depth of over 2,000 meters.

The Rich South Sea

The South Sea is located in the tropical and the subtropical zones, and at the same time it is within the region of monsoon activity. Therefore the southwesterlies blow in the summer and the northeasterlies blow in winter.

But the general wind direction is consistent with the northeast to southwest direction of the South Sea. This is an important natural geographical characteristic of this oceanic region which affects changes in oceanic currents and ocean water temperatures. The hydrological circumstances possess obvious deep oceanic characteristics, and seasonal changes are also very visible. In winter, the lowest water temperature of the surface layer of the sea along the coastal regions is 18°C and in the mid sea area it is 28°C. In summer, the highest water temperature at the surface of the sea reaches about 29°C. Because seasonal changes also affect changes in salinity, therefore during the northeasterly monsoon season, the effects of dryness and cold increase the amount of evaporation from the surface of the sea and the amount of rainfall at this time is also relatively small and thus the salinity of the entire region of the sea rises. During the southwesterly monsoon period in summer, the amount of rainfall during this period increases and runoff also increases, forcing the salinity of the surface layer of the entire region of the sea to universally drop. Seasonal changes also bring about different biological foods of different periods. This provides a superior material condition for the reproduction and propagation of oceanic life forms. Therefore there are plenty of varieties of life forms in the South Sea.

But the total amount of living matter is not high. Seasonal change is not great. A single peak period occurs in a year generally in winter and spring. For example, the total amount of living matter of lowly productive plankton in the Xisha and Zhongsha Archipelagos is between 30 and 30 milligrams/m^3, 66 milligrams/m^3 in the northern continental shelf of the South Sea, while in Donghai it is 120 killigrams/m^3. In Donghai, two peaks occur in a year in spring and autumn and the difference between the highest and lowest is 10 to 30 times, while in the South Sea the difference is only 2 to 5 times. Superior varieties are more visible in Donghai and the proportion is greater. In the South Sea they are less visible and their proportion is small.

The region of oceanic living matter in the South Sea belongs to the Indian-western Pacific region, the southern and the central parts belong to the Indonesia-Malaysia subregion possessing tropical characteristics, and the northern part belongs to the China-Japan subregion. There are tropical sea turtles, hawksbills, spear fish that can rapidly swim back and forth,

sword fish, fishes of the coral reefs that swim slowly such as the ugly scorpion fish and the beautiful butterfly fish, horseshoe shells (gaolai shellfish), mollusks and beautiful shells as well as sea cucumbers, lobsters, crabs, and octopi which live in coral reefs. There are also many ocean vegetation. Unique to the Dongsha Archipelago is Caloglossa leprieurii, a kind of red algae used to eradicate roundworms.

In the South Sea, individual ocean life forms participate in the development of the landform and the soil. Many shapes and sizes and varieties of coral polyp deposited their own bones to construct the bright pearls of the green sea--coral reefs. The islands of the South Sea of our nation are composed of over 200 such sinking or floating coral reefs. In the clear regions of sea water around the South Sea are also scattered coral reef coasts peculiar to the tropics. Along the coasts of muddy and unclear waters, a coast of mangroves peculiar to the tropics has developed. The mangroves are dense in the south but sparse in the north. There are 43 species in Malaysia. There are only 18 species on Hainan Island in our nation, such as mulan, hailian, jiaoguomu, qiujia, hongjiadong, and haiqi.

Sea birds and coral affect the development of soil on the coral island. A phosphorous limestone soil entirely different from latosol of the tropics is formed which is rich in calcium, phosphorus, nitrogen and salt. A coral reef vegetation is formed on this special kind of soil and transforms the coral islands into green oases. Plant life on the islands possess resistance to dryness, the leaves (and even the entire plant) are fleshy, the tree trunks have a lot of pith (hallow) and break easily. Because the soil lacks iron, manganese and such trace elements, plants suffer from chlorosis.

There are coconut trees planted by man on the coral islands. Coconut trees can serve as navigational marks. They have become the symbol of coral islands. The islands are also rich in tropical fruits such as papayas, mangos, bananas, pineapples, etc. There are also flocks of ibises and birds that prey on bonitos. The sea has an even richer store of life forms. There are schools of fishes, the large shining and bright red fish that are very attractive to man, tasty and fresh lobsters. Although coral reefs are hindrances to sailing in the ocean, they are indeed warehouses of various aquatic products. The many shapes and forms of coral and the colorful shells on the beaches are not only important decorations but also are valuable as industrial raw materials.

The ocean is also a treasure box of chemical resources such as table salt which is not only necessary to life but also an important raw material of the chemical industry. The Yingehai at the southern tip of Hainan Island is a large and world famous salt field. Someone has estimated that in one cubic kilometer of sea water there are over 27 million tons of sodium chloride (table salt). It can be used for the extraction of magnesium chloride, light magnesium oxide and metallic magnesium which are all important raw materials necessary for construction of industry and agriculture, poineer sciences and national defense construction. They are

tremendous riches for our building of socialism. The South Sea is also one of the regions with the largest deposits of natural gas and petroleum.

The mineral resources at the bottom of the South Sea are also rich in tungsten, tin, lead, gold, zircon, monazite, titanium and iron ore and rare elements of niobium, tantalum and thorium contained in pelagic sediments. They have provided a bright future with wide possibilities for prospecting of the sea floor in the near future.

The temperature differential on the surface of the South Sea can also be used to generate electricity. Here there are superior natural conditions that have great potential.

We believe that our nation's expansive South Sea will be able to develop greater functions under the glorious goals of hastening building of our nation's four modernizations under the Party Central Committee led by Chairman Hua.

9296
CSO: 8111/0472

APPLIED SCIENCES

SUDDEN WESTWARD TURNS OF TYPHOON PATHS OVER EAST SEAS ANALYZED

Beijing DAQI KEXUE [SCIENTIA ATMOSPHERICA SINICA] in Chinese Vol 3 No 3, Sep 79 pp 289-297

[Article by Chen Lianshou [7115 5114 1108] of the Central Meteorological Observatory: "Casual Analysis of Sudden Westward Turns of Typhoon Paths Over the Seas of Eastern China"--This article was received on November 15, 1977]

[Text] Abstract

The sudden westward turn of typhoon paths over our nation's eastern seas (Huanghai and Donghai) is an abnormal path that cannot be easily forecast accurately. Since 1970, this kind of path has occurred six times, five of which were sudden and unexpected attacks upon the eastern regions. At present, the various statistical and dynamic forecasting methods used by our nation and foreign nations generally could not forecast this kind of abnormal path. This article analyzed the causes of the westward turns of the six typhoons. The analysis showed that there were six causes of westward turns of typhoon paths. Among these, the effect of attraction by the cold cutoff eddy was a frequently seen and basic cause. This article's conclusions provide a better reference for forecasting operations in the prediction of this type of typhoon.

I. Introduction

The absolute majority of typhoons that move northward over the eastern seas of our nation turn toward the northeast during their later course. Only a very few typhoons suddenly turn westward and blow overland of our nation. The path of this kind of sudden westward turn frequently cannot be forecast. This has brought about sudden attacks upon our nation's eastern seas and coast, causing bodily harm and death and loss. Since 1970, there had been a total of six such typhoon paths that suddenly turned westward over Huanghai and Donghai. Five of these occurrences were not forecast in time and preparations were not made in time. Eastern regions suffered different degrees of damage.

The sudden westward turn of typhoon paths over the eastern seas of our nation is a kind of abnormal typhoon paths. At present, forecasting abnormal paths is one of the problems that the forecaster finds the most difficult. This kind of path of sudden westward turn has a very small probability of occurrence. Sometimes the path's angle of deviation from the leading air flow is great. Because of these two characteristics, the dynamic method of forecasting based on the principle of lead and the statistical method based on historical samples become ineffective in forecasting this kind of paths.

This article analyzed the course of sudden change in the peripheral fields of air flow of the typhoons at the time the six westward turns of the typhoon paths occurred over the eastern seas, and pointed out the main cause of this kind of westward turn.

II. General Characteristics

The typhoon paths that turns westward over our nation's eastern seas can be divided into two types: One is the path of westward turn over Huanghai. The typhoon lands on the Shandong Peninsula or the coast north of it. The second is the path of westward turn over Donghai. The typhoon lands at the mouth of the Changjiang and the coast of southern China south of it. The occurrence of these two types of paths possesses visible seasonal characteristics. Table 1 shows the frequency of occurrence of the path of westward turn over Huanghai. Numbers in parentheses are the percentages of such paths of westward turns among the total number of typhoons that occurred in that particular month over the years for which statistics were recorded. Paths of westward turn over Huanghai occurred only in the 3 months of June, July and August, and they were most concentrated in July. Table 2 shows the frequency of occurrence of the paths of westward turn over Donghai. Paths of westward turn over Donghai occurred in July, August and September, and the highest frequency occurred in August.

Table 1. Monthly Frequency of Typhoon Paths of Westward Turn Over Huanghai 1949-1974

Month	Jan-May	June		July		August		Sep-Dec
		No	Per-cent	No	Per-cent	No	Per-cent	
Frequency	0	1	(1.9)	5	(4.5)	1	(0.6)	1

Table 2. Monthly Frequency of Typhoon Paths of Westward Turn Over Donghai 1884-1977[1)]

Month	Jan-May	June		July		August		Sep-Dec
		No	Per-cent	No	Per-cent	No	Per-cent	
Frequency	0	5	(1.3)	11	(2.5)	5	(1.2)	0

1) Part of the statistics was prepared by Du Shunyi [2629 7311 5030] and Lu Peizhi [0712 1014 1807] graduates of the class of 1977 of Beijing University

The localities of sudden westward turns of typhoons over the eastern seas of our nation also showed a relative concentration (Figure 1). Figure 1 was drawn from the distribution of points of westward turns shown in the years of statistical records used in Tables 1 and 2. The distribution of westward turns of the typhoon paths over Huanghai was over the sea and region near Korea's Jizhou Island. The distribution of westward turns of typhoon paths over Donghai was on the two sides of the central and western parts of the Ryukyu Islands.

Before and after the points of westward turns the moving speed of the typhoons visibly showed discontinuity. After the point of westward turn, the typhoon suddenly increased its moving speed and even "hopped." For example, typhoon No 7203 that turned westward over Huanghai moved at 32 kilometers/hour before it turned westward. After it turned westward its moving speed reached 74 kilometers/hour. Within 6 hours, it moved from over the sea near Jizhou Island to over the sea near Chengshantou on the Shandong Peninsula of our nation. Again for example, typhoon No 7504 that turned westward over Donghai moved at 15 kilometers/hour before it turned westward. After it turned westward, it reached a moving speed of 30 kmph. The sudden westward turn of the typhoon path and this type of acceleration of the moving speed after turning westward often catch the coastal regions off guard, preparations could not be made in time, and thus cause damage and loss.

III. Analysis of Several Individual Cases

We analyzed the six typhoon paths that suddenly turned westward in recent years. Figure 2 shows the paths of these six typhoons. These paths were all moving from over our nation's eastern seas toward the north at first and then they suddenly turned westward.

(Case 1) A typhoon not assigned a number which occurred between June 12 and 16 in 1970

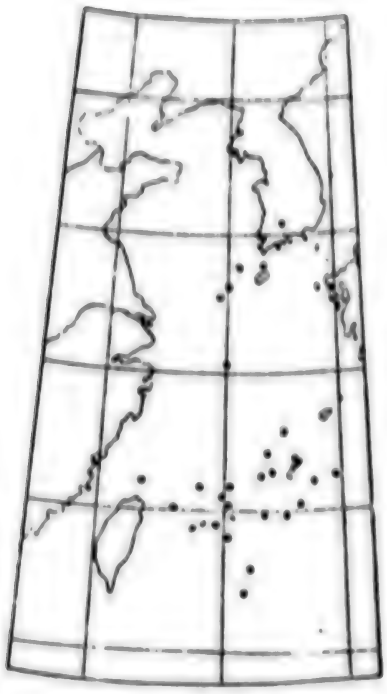

Figure 1. Geographical Distribution of the Points of Westward Turns Over the Eastern Seas [1)]

1) Part of the statistics was prepared by Du Shunyi [2629 7311 5030] and Lu Peizhi [0712 1014 1807] graduates of the class of 1977 of Beijing University

This typhoon was formed on June 11 over the northeastern part of Nanhai. Before June 14 it moved toward the northeast and at the time meteorological departments of various concerned nations forecast that this typhoon would continue to move in a northeasterly direction. But on June 14, the midlatitude circulation along the coast of East Asia suddenly changed and a strong blocking high pressure system was formed over our nation's northeastern region and at the same time a cold eddy appeared in the cutoff of the high altitude trough over eastern China (Figure 3). At this time, the typhoon was situated over the sea near Jizhou Island. The typhoon was very close to the cold eddy to its west (about 7° latitude apart). After 0020 hours on the June 14, this typhoon was led by the southeasterly airflow between the blocking high pressure system and the cold eddy and suddenly changed course toward the northwesterly direction and moved to over the sea near our nation's Qingdao Peninsula. At the same time the typhoon combined with the cold eddy, changing the typhoon into a cyclone of the

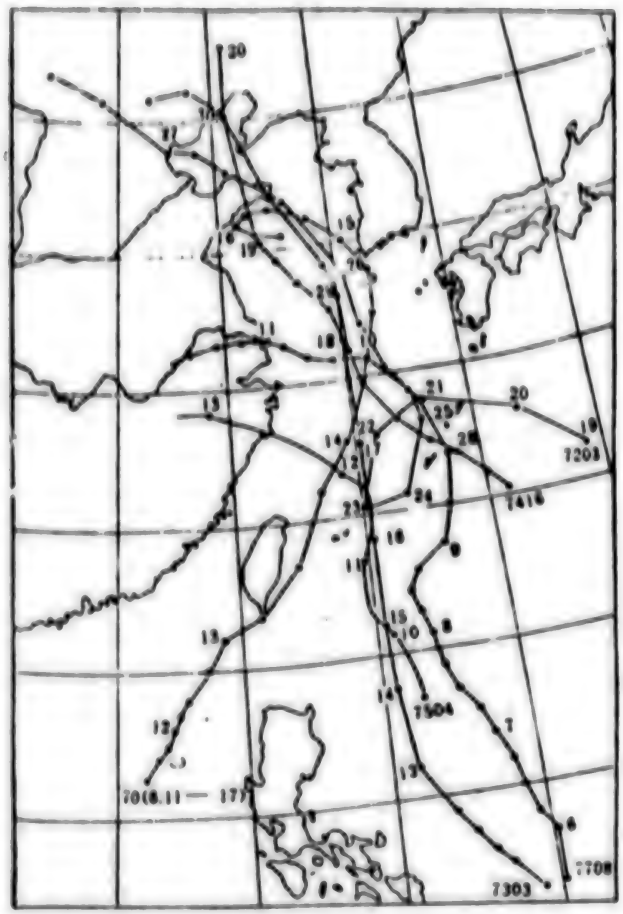

Figure 2. The six typhoon paths that turned westward

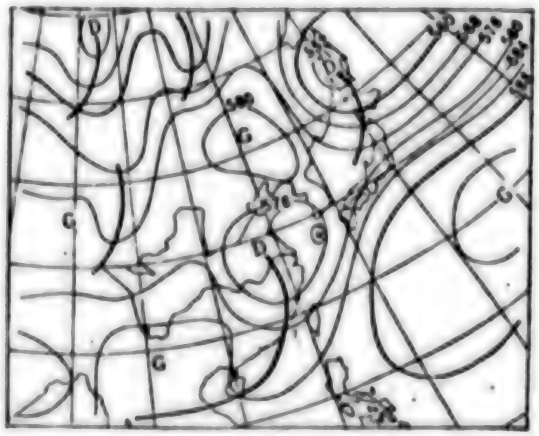

Figure 3. Altitude field of 500 millibars at 2000 hours on June 14, 1970

temperate zone and its intensity visibly increased. The coastal regions of our nation's Liaoning and Shandong provinces and Bohai and northern Huanghai suddenly were attacked by winds of 11 on the Beaufort Scale.

(Case 2) Typhoon No 7203

This typhoon was formed over the sea near Guam on July 5. After 3 rotations and moving over the sea for 20 days, it moved to over our nation's eastern sea on the 25th and then shifted in a northerly direction. At 0800 hours on the 26th, it moved over the sea near Jizhou. At this time, the typhoon was situated in front of a deepening long wave trough (Figure 4a). At the time, concerned nations' meteorological departments all forecast this typhoon would move in a northeasterly direction. But at this time a sudden change occurred in the type of flow over East Asia (Figure 4b). The deep trough over the eastern part of China broke into two. The southern part became a cold cutoff eddy; the northern part underwent a shallow trough contraction. The subtropical high pressure (whose main body was over the Japan Sea) extended westward in the breaking zone. The typhoon, led by the strong southeasterly winds between the subtropical high pressure ridge and the cold cutoff eddy, suddenly turned toward the northwest and accelerated its movement. When this typhoon turned westward, it similarly combined with the lower layer cold eddy to the west and strengthened, and the coast of our nation's Liaoning and Shandong provinces, Bohai and the northern part of Huanghai again were suddenly attacked by strong winds and stormy rains.

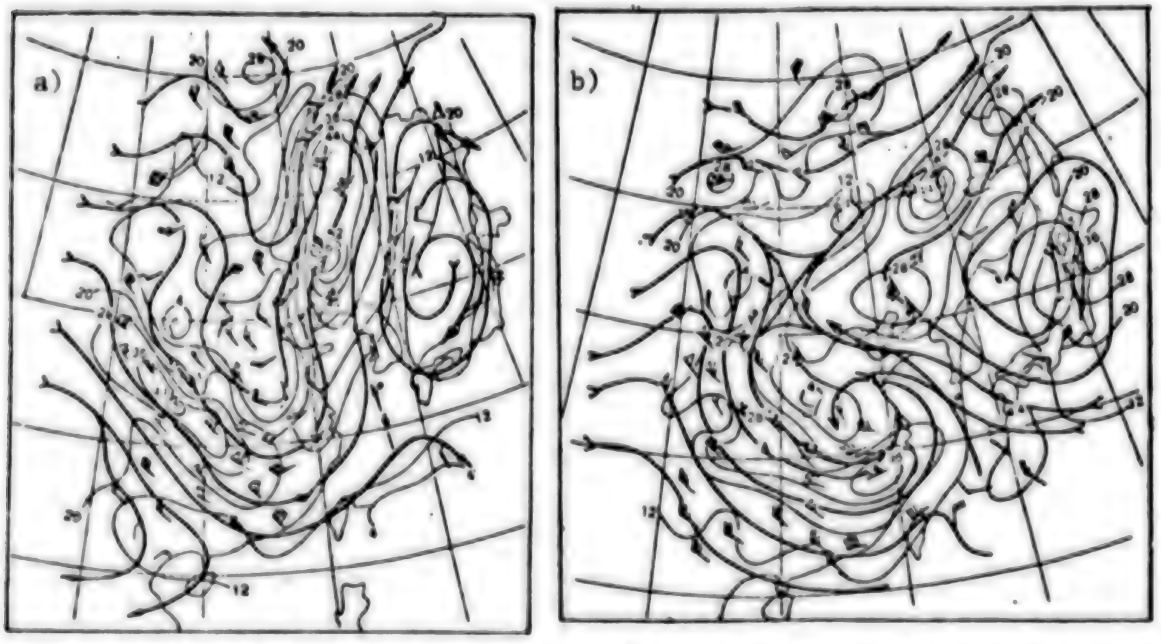

Figure 4. Sudden situational change at the time of westward turn of Typhoon No 7203

a) Field of air flow at 300 millibars at 2000 hours on July 25
b) Field of air flow at 300 millibars at 2000 hours on July 26

The fine solid lines are isanemones

(Case 3) Typhoon No 7303

This typhoon formed over the ocean east of the Philippines on July 13 and then basically moved along 125°E longitude toward due north. By the 18th it had moved to over the sea southwest of Jizhou Island. At this time, typhoon No 7304 appeared to the southwest 6° to 7° latitude from the first. Due to the circling movement of the dual typhoons[1] [2], typhoon No 7303 turned westward (Figure 5) and landed on the Shandong Peninsula. Typhoon No 7304 landed over central Guangdong on the 17th. After landing it turned and moved toward the northeasterly direction and approached typhoon No 7303.

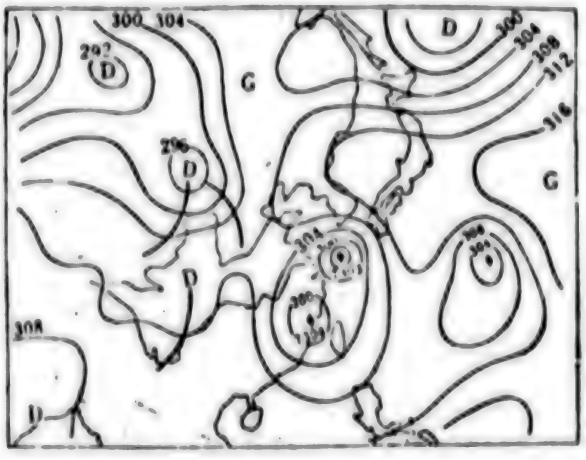

Figure 5. Altitude field at 700 millibars at 0800 hours on July 18, 1973

(1) Brand S., 1970, The interaction of binary tropical cyclone on the Northwest Pacific Ocean, J of Applied meteor. Vol 9 No 3

(2) Haurwitz, B., 1951, The motion of Binary tropical cyclone, Archir Für Meteorologie Geophysik and Bioklimatologe, Series A, Band 4

(Case 4) Typhoon No 7416

This typhoon was formed on the night of August 27. At 2000 hours on the 28th the typhoon weakened in intensity. At 0800 hours on the 29th, the circulation of the lower layer of the typhoon was attracted by a cold eddy to the northwest and the two combined. The middle layer was led by the peripheral southeasterly airflow of the cold eddy in the deep trough over the eastern coast of our nation and turned toward a northwesterly direction (Figure 6) and accelerated. Because of the invasion of cold air and the combination with the cold eddy, this weakened typhoon changed speed and developed into a very strong cyclone of the temperate zone over Huanghai[3].

(3) Ren Zejin [0117 3419 0689], Yuan Xinxuan [5913 0207 6513], Chen Longxun [7115 7127 8113], Shen Rujin [3088 1172 6855], Yang Yibi [2254 5030 4310], and Chen Lianshou [7115 5114 1108], 1979, The Processes of Change of Typhoon No 16 of 1974 from Weakening and a Change in Characteristics to the Development Into a Cyclone of the Temperate Zone.

Our nation's northern coast was suddenly attacked for the third time by winds of 10 to 12 on the Beaufort Scale.

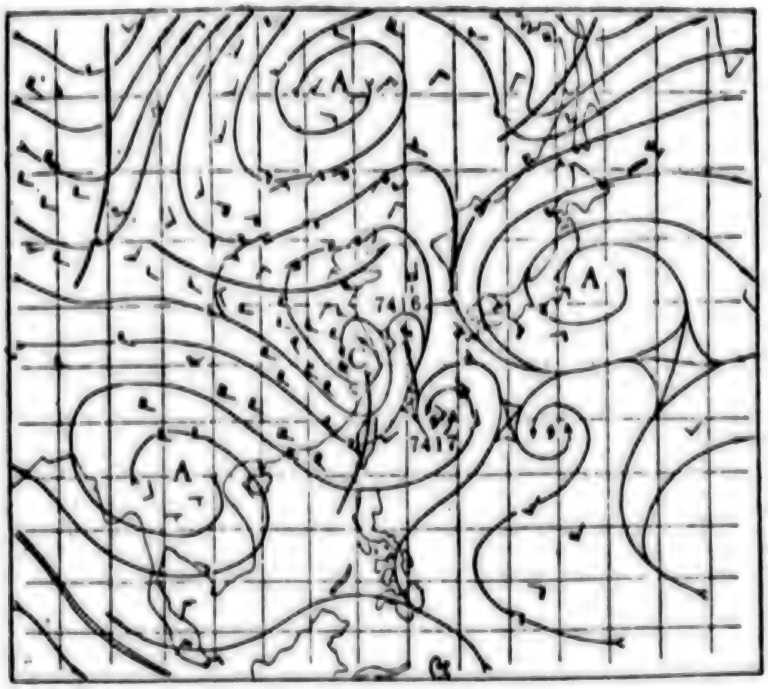

Figure 6. Airflow line chart at 500 millibars at 0800 hours on 29 August 1974

(Case 5) Typhoon No 7504

This is a typhoon that suddenly turned westward over Donghai. This typhoon was formed over the sea southeast of our nation's Taiwan Province on August 10 and moved in a northerly direction. On the 11th, the typhoon moved to over the sea near the southwest of Okinawa. At this time a cold eddy was first located on the north side of the typhoon but later it moved toward the southwest to the west side of the typhoon (Figure 7) and the distance between the 2 shortened to between 7° and 8° latitude. Because the cold eddy visibly attracted the typhoon and caused a circling effect, typhoon No 7504 suddenly turned westward and finally landed at Wenling in Zhejiang Province.

(Case 6) Typhoon No 7708

This typhoon was formed over the western Pacific on 2 September. After the 6th it moved northward and by the 10th it had moved to over Donghai. On 8 September, a cold eddy emerged as a cutoff eddy from the region over the Korean Peninsula and inside the deep trough over the Japan Sea. Later the cold eddy moved in a southwesterly direction to the west side of the

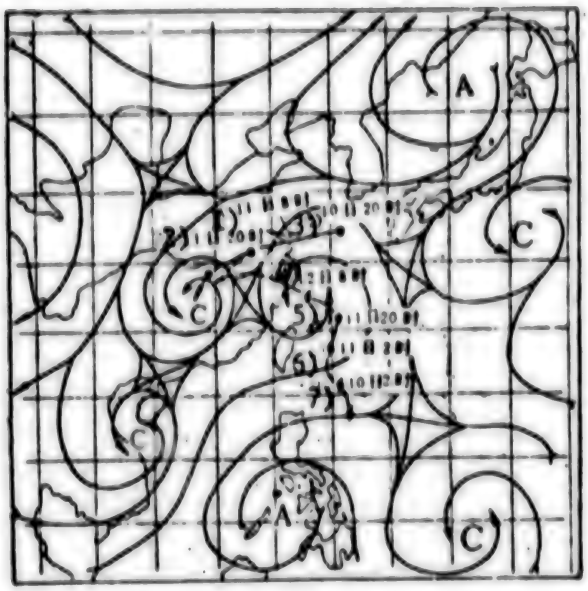

Figure 7. Airflow line chart at 500 millibars at 0800 hours on 12 August 1975. Black round dots mark the path of the cold eddy

Key:
1) 0800 hours, 11th
2) 2000 hours, 11th
3) 2000 hours, 10th
4) 0800 hours, 12th
5) 2000 hours, 11th
6) 0200 hours, 11th
7) 0200 hours, 10th

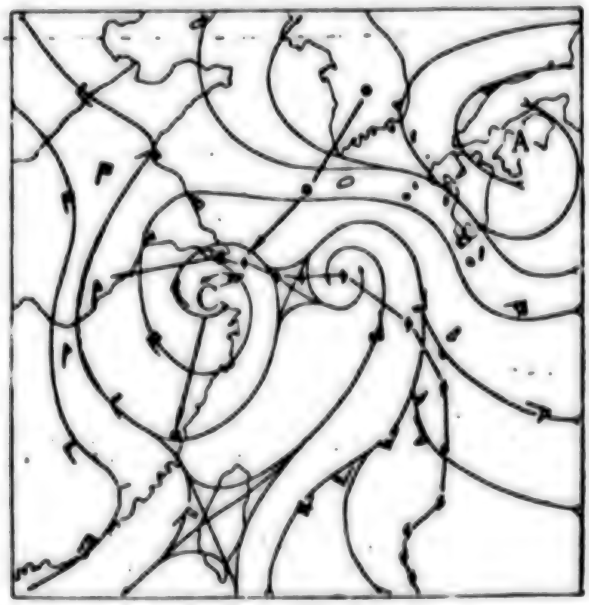

Figure 8. Airflow line chart at 200 millibars at 0800 hours on 10 September 1977. Black round dots mark the path of the center of the cold eddy. Typhoon symbols mark the path of the center of the typhoon.

typhoon. On 8 October, the cold eddy had reached the location 4° latitude west of the typhoon (Figure 8). On September 20, the typhoon was attracted by the cold eddy situated to its northwest and moved in a northwesterly direction. On 8 October, the effects of the cold eddy to the west-southwest of the typhoon caused typhoon No 7708 to suddenly turn westward. Shanghai City, where very few typhoons land, directly suffered a sudden attack by this typhoon.

Of these six individual instances of sudden westward turns which we analyzed, five cases were related to cold cutoff eddies at high altitudes. The other case was due to the mutual effects of dual typhoons. Thus, it can be seen that high altitude cold cutoff eddies are closely related to the sudden westward turn of typhoons over the eastern seas. It can be seen from the analysis of the above cases that the blocking high pressure system over the northeastern region of our nation, the intensification of the subtropical high pressure ridge from its westward extension at the cutoff point of the cold eddy and the effects of dual typhoons are all related to the sudden westward turn of typhoons over the eastern seas.

IV. The Causes of Sudden Westward Turns of Typhoon Paths

Analysis of the six cases of typhoon paths of westward turns and of other cases indicates, the author believes, that there are the following six reasons for the sudden westward turns of typhoon paths:

(1) The Effect of High Altitude Cutoff Eddies

When a cold eddy is cut off in the deep trough of the peripheral belt of westerlies of a typhoon, circulation of the cold eddy will cause a sudden change in the field of airflow surrounding the typhoon and cause the typhoon to make a sudden turn. The high altitude cold eddy exerts two effects upon the path of the typhoon, a leading action and attraction.

The leading action occurs when the circulation of the high altitude cold eddy spills over into the typhoon area. At this time the movement of the center of the typhoon will be led by the peripheral field of airflow of the cold eddy. The direction of movement will basically be consistent with the direction of the peripheral airflow of the cold eddy. The leading effect of the peripheral airflow of the cold eddy upon the typhoon is frequently manifested in three ways (Figure 9): When the cold eddy is situated to the northeast of the typhoon, the peripheral airflow of the cold eddy will force the typhoon to move southward (Figure 9a). For example when typhoon 7204 approached the area near Shantou, the center of the typhoon, was above the mouth of Changjiang to the northeast. Suddenly a high altitude cold eddy was cut off from the deep trough and emerged, and one branch of the easterly airflow south of the subhigh which had been dominant over the center of the typhoon changed to a peripheral northerly airflow of the cutoff cold eddy after this eddy emerged. Under the lead of this branch

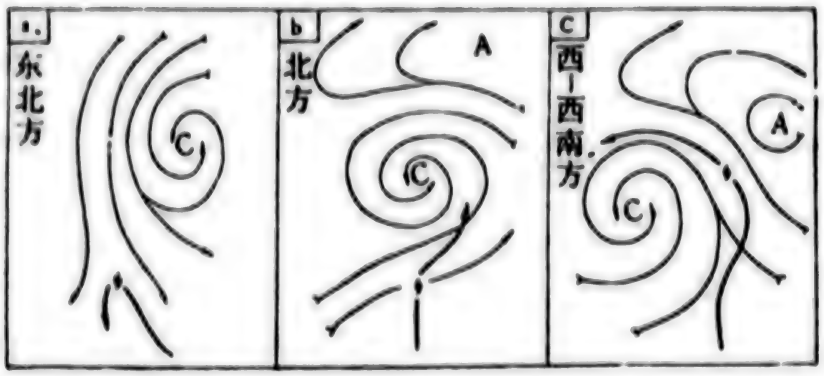

Figure 9. Three positions of the leading effect of the cold eddy

a) northeasterly direction
b) northerly direction
c) west-southwesterly direction

of northerly wind, the center of the typhoon which was originally moving in a northwesterly direction suddenly turned and moved toward a southerly direction and did not land at Shantou. This high altitude cold eddy caused typhoon No 7204 to finally form an extremely complex and abnormal path. When the cold eddy was situated to the north of the typhoon (Figure 9b), the peripheral westerly wind south of the cold eddy tended to make the typhoon move toward the east. Due to the effects of inner forces of the typhoon, the actual path of the typhoon moved in a northeasterly direction. When the high altitude cold eddy was situated to the north of typhoons No 7504 and 7708, a consistent path of northward movement slanting toward the east emerged. When the cold eddy was situated to the west or the southwest of the typhoon (Figure 9c), the typhoon was led by the peripheral southeasterly airflow to the east or the northeast of the cold eddy. This caused the typhoon to move toward the northwest or toward a westerly direction. When the paths of the typhoons over our nation's eastern seas suddenly turned westward, there frequently existed a high altitude eddy to their west or southwest. Figure 10 shows the movement of typhoon No 7708 relative to the cold eddy taking the center of the cold eddy as the point of origin. The leading effect of the field of peripheral airflow of the cold eddy upon the movement of the typhoon can be seen.

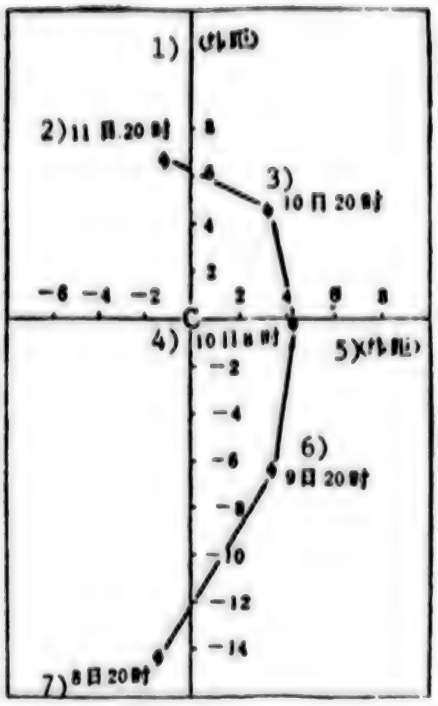

Figure 10. Path of relative shift of the center of typhoon No 7708 to the center of the cold eddy

Key: 1) (latitudinal distance)
2) 2000 hours on the 11th
3) 2000 hours on the 10th
4) 0800 hours on the 10th
5) (latitudinal distance)
6) 2000 hours on the 9th
7) 2000 hours on the 8th

When the distance between the cold eddy and the typhoon shortened sufficiently, the two appeared to exert mutual attraction. The total pressure of the effect upon the cylindrical boundary surface of the typhoon can be written as:

$$\oint_{\sigma} Pd\sigma = \iiint_{\tau} \nabla Pd\tau$$

Let the semicylindrical boundary surface near the cold eddy be σ_1, the back side be σ_2, then when the cold eddy and the typhoon approach each other sufficiently the σ_1 side's atmospheric pressure gradient force will visibly lessen, and thus

$$\oint_{\sigma_2} Pd\sigma \gg \oint_{\sigma_1} Pd\sigma$$

The typhoon is pushed toward the cold eddy and even combines with the cold eddy. This is the effect of attraction of the cold eddy. In actual synoptic processes, when the cold eddy moves to the northwest or the west of the typhoon, it is the time when the cold eddy and the typhoon are the closest in distance in the course of the movement of the cold eddy. The cold eddy visibly attracts the typhoon, forcing the typhoon to violently jump toward the position of the cold eddy--toward the northwesterly direction.

The attraction and combination processes of the cold eddy and the typhoon were frequently manifested in the middle and lower layers of the troposphere. This was shown on the satellite cloud maps as a combination of two cloud masses. The cloud mass that was formed by the combination frequently showed a clearer spiral structure. This indicated that the systems resulting from the combination generally all show visible intensification, or cause a change in the nature of the original typhoon to become a strong cyclone of the temperate zone.

The effects of the cold eddies upon the moving speeds of typhoons showed greater differences under the three situations illustrated in Figure 9. The leading effect of the peripheral airflow of the cold eddy shown in Figure 9a and the internal forces of the typhoon were two factors that were completely opposite to the effect of the typhoon's shift in direction or canceled the effect of the typhoon's shift in direction. The typhoon's moving speed was the slowest under the influence of the cold eddies. In Figure 9b, the moving speed was the next slowest. Therefore, the two kinds of effects described above did not entirely cancel out. Figure 9c showed the typhoon accelerated violently. When the cold eddy was cut off and moved in a southwesterly direction,[1] the easterly wind of the southern part of the subtropical high pressure system originally east or north of the cold eddy again stayed close to the typhoon and exerted a leading effect. Thus, at this time, the four leading effects of the cold eddy upon the airflow, the subtropical high pressure upon the airflow, the inner forces of the typhoon (northwesterly) and the attraction of the typhoon by the cold eddy were all in the same direction and all consistently pushed the typhoon toward the northwesterly direction. This was the reason for the abnormal acceleration of the movement of the typhoon when it turned westward.

(2) High Altitude High Pressure System of the Northeastern Region of Our Nation

The second basis for determining if a typhoon turns westward above the eastern seas is to observe whether there is a high pressure zone or westerly jet stream zone above our nation's northeastern region. The westerly jet streams appear over our nation's northeastern regions. The typhoon that moves to Huanghai is not likely to turn westward. When a blocking high

---

1) The path of the midlatitude high altitude cold cutoff being led by a northeasterly or easterly air flow generally progresses in a southwesterly direction.

pressure or a relatively strong high pressure ridge occurs, an easterly or a southeasterly airflow will prevail over the northern part of Huanghai and Bohai and will cause the typhoon to turn and move in a northwesterly direction.

Sometimes a high altitude high pressure system over the northeastern region already exists when forecasting whether a westward turn by a typhoon will or will not occur over our nation's eastern seas. For example, in (Case 1), a blocking high pressure system had already been established above the northeast when the typhoon moved in a northeasterly direction. When the typhoon approached the southern part of this blocking high pressure system, it visibly strengthened this high pressure system. This is an important basis for forecasting a westward turn by the typhoon. But sometimes formation of this high pressure system and the westward turn of the typhoon occur almost simultaneously. This is the result of a sudden change in the situation. This high pressure was formed at the breaking point of the deep trough (north of the cutoff cold eddy). At this time, forecasting a westward turn by the typhoon must be based on estimates of adjustment of the situation.

(3) The Effect of Wind Storms of the Bay of Bengal Upon Westward Turns

In midsummer all westward turns of typhoons over the eastern seas require an intensified westward extension of the subhigh. Wind storm activity of the Bay of Bengal is a method of intensifying the westward extension of the subhigh over our nation's eastern seas, and not enough attention has been given to this method.

When a relatively strong wind storm of the Bay of Bengal lands, the situation of the upper layer of the troposphere over the Qinghai-Xizhang Plateau will undergo a kind of sudden change. At this time, a deep long wave trough resulting from the combination of the westerly trough and the wind storm of the Bay of Bengal may be established over the plateau. The lower reaches of the half wave length (our nation's eastern seashore) will be the place for the establishment of the long wave ridge. At this time, the subtropical high pressure ridge over our nation's eastern seas will intensify and extend westward. If at the same time there is a typhoon moving north, the typhoon will turn westward on the south side of the subhigh. The westward movement of typhoon No 7413 was such a case. Between August 15 and 16, a relatively strong wind storm of the Bay of Bengal landed and combined with a trough originally over the Balkhash Lake over the Qinghai-Xizhang Plateau to form a deep long wave trough with a large amplitude. The high pressure system originally over the Qinghai-Xizhang Plateau was forced to move in a northeasterly direction, creating a dynamic anticyclone at 500 millibars above the northeastern region of China. It is the result of the combination and intensification (negative vorticity reached 87) of the eastward moving Qinghai-Xizhang high pressure system and the subtropical high pressure system. This kind of sudden change caused typhoon No 7413 situated over

Donghai to move due west (Figure 11), and on the night of the 19th the typhoon landed over the northern part of Zhejiang Province.

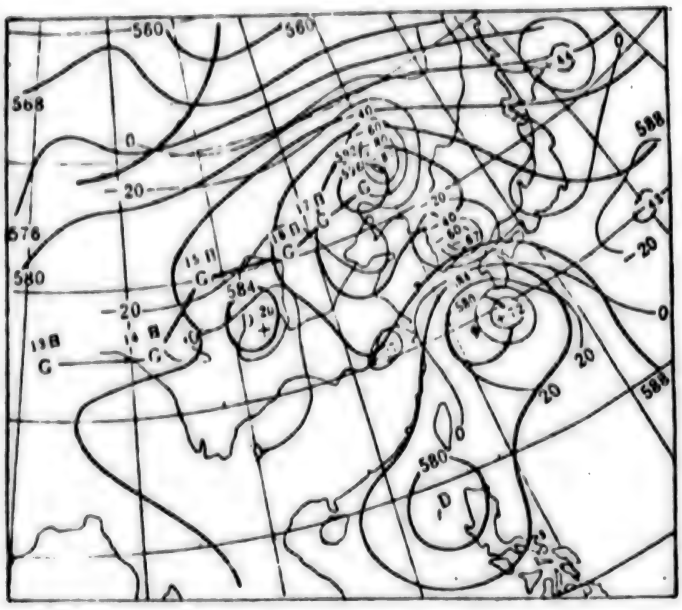

Figure 11. The altitude field at 2000 hours on 18 August 1974. The arrow indicates the path of the center of the Qinghai-Xizhang high pressure system. The fine solid line shows the distribution of voticity at 0800 hours on the 18th (unit 20 x 10^{-6}/sec)

We compiled statistics on the relationship between the wind storm activities of the Bay of Bengal[1)] and the typhoon paths over the western Pacific for the years 1961-1970 (Table 4) and discovered that when there were windstorm activities in the Bay of Bengal, 93 percent of the corresponding typhoons over the western Pacific moved west in midsummer and 94 percent moved west in autumn and winter.

Table 4. Path of Typhoons Over the Western Pacific During the Period of Windstorm Activity of the Bay of Bengal 1961-1970

Month	Jan-June	Jul-Sep	Oct-Dec	Total
Corresponding number	5	28	18	51
Westward shift	2(40%)	26(93%)	17(94%)	45(88%)
Direction of turn	3(60%)	2(7%)	1(6%)	6(12%)

1) Reference not given

(4) The Effects of Dual Typhoons

The effects of dual typhoons are also one of the causes of westward turns of typhoons over the eastern seas. When another typhoon approaches the south side or the southwest side of a northward moving typhoon over the eastern seas, the counterclockwise circling movement between the dual typhoons will cause this typhoon's path to turn westward. Since 1970, at least three westward turns of typhoons 7009-7010, 7203-7204, 7416-7417, were related to the effects of dual typhoons.

(5) Asymmetric Structure and Nongeostrophic Effects

The particular distribution of atmospheric pressure fields over our nation's eastern seas also exert two visible effects upon the westward turns of northward moving typhoons over the seas. The first effect is caused by the asymmetric distribution of wind speeds within the range of the typhoon. The northward moving typhoon over the eastern seas frequently neighbors the subtropical high pressure system on the east side, and its western part neighbors the subtropical high pressure system on the east side, and its western part neighbors the deep trough over our nation's coast. Thus, in a few cases in which the high pressure system is strong and the trough is deep, the gradient of atmospheric pressure will cause a far higher wind speed in the eastern and western circulations of the typhoon than the wind speed in the western and southern half. The difference between the two is great and thus the typhoon is led into a westward turn.[1)] This type of windspeed distribution can be seen on the weather map. The isobars of the typhoon cluster to the northeast and disperse to the southwest, forming an off center of the typhoon slants to the northeast side.

1) The relationship between the distribution of wind speed and the speed of movement of the typhoon is

$$C_x = 1/2\ (u - u' - 4\ QR\sigma \frac{2}{P} \cos \bar{\varphi}) \quad C_y = 1/2\ (v - v')$$

where C_x, C_y are respectively the components of the moving speed of the typhoon in the east-west direction and the south-north direction. Movement eastward and northward are positive. u, v are the components of the normal values of windspeed of the typhoon (i.e., westerly wind and southerly wind), u', v' are negative valued components (easterly wind and northerly wind), $\bar{\varphi}$ is the average degree of latitude within the range of the typoon, σ is the radius of the typhoon (latitudinal distance), R is the radius of the earth, Q is the speed of spin of earth. Because of the distribution of atmospheric pressure, $v > v'$, $u < u'$, thus $C_x < 0$, $C_y > 0$, making the typhoon turn and move in a northwesterly direction.

The second effect is caused by the uneven isohypses of a north-south direction over our nation's eastern seas. This kind of isohypses has a large gradient in the north and a small gradient in the south. When the typhoon is led by a branch of southerly airflow into a northward movement over the eastern seas, the typhoon will move from the dispersed region of the isohypses (where the speed of the leading airflow is small) toward the clustered region of isohypses (where the speed of the leading airflow is large) (Figure 4a). Thus, a nongeostrophic effect is exerted upon the leading activity that precedes the typhoon. This kind of nongeostrophic effect will cause the point eddy of the typhoon that is moving northward to shift to the clustered region of isohypses of the basic atmospheric pressure field, and the point eddy will turn toward the side of low pressure (the westward turn) and create acceleration. This is the result of geostrophic equilibrium and adaptation processes of the point eddy of the typhoon inside this type of large scale basic atmospheric pressure field.

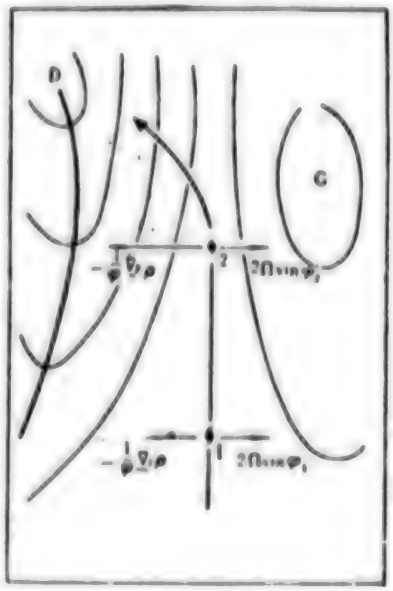

Figure 12. The nongeostrophic effect during the typhoon's northward movement

The authors thank Mr Tao Shiyan [7118 6108 6056] for contributing his precious comments and Comrade Zhang Shurong [1728 2885 2837] for drawing the illustrations.

9296
CSO: 4008

APPLIED SCIENCES

OBSERVATION OF SUNSPOT ACTIVITY STEPPED UP

Effect on Weather Studied

OW141440 Beijing XINHUA Domestic Service in Chinese 1558 GMT 12 Apr 80 OW

[Summary] Beijing, 12 Apr--"Does sunspot activity have any effect on the weather? A survey conducted by Chinese meteorologists of the 72 chromospheric explosions (also known as solar flares) that occurred over the last 40 years when big black sunspots appeared gives the answer. Within 1 month following a chromospheric explosion, the surface temperatures of many localities of China apparently increased by an average of 0.5 to 1 degree centigrade."

The frequent bursts of solar flares at present are due to the fact that sunspot activity is at the peak of 11-year cycle. Changes in sunspot activity represent changes in the sun's total radiation.

"The relationship between sunspot activity and precipitation is rather complicated. Through many years of observation, China's meteorologists have discovered that rainfall in north China is usually greater than normal around the time when sunspot activity is at a peak and is usually scarce in years when sunspot activity reaches the maximum. But this is not so in the lower reaches of the Changjiang [Yangtze] River where the rainy season comes in the year when the sunspot activity reaches a maximum."

Sunspot activity has an approximate 11-year cycle. The period from August 1979 to February 1981, the peak year of solar activity, has been internationally acclaimed for solar study. More flares and sunspots will be observed during this period. Chinese astronomers are taking this opportunity to conduct a number of observations and studies.

Major Sunspot Groups Observed

OW111208 Beijing XINHUA in English 1200 GMT 11 Apr 80 OW

[Text] Kunming, April 11 (XINHUA)--Two huge groups of sunspots, not far away from each other, have now passed from the centre of the solar face and are moving to its western hemisphere, according to the Yunnan observatory, centre of observation of solar activity in southwest China.

They are expected to disappear into the western edge of the solar face on April 14 and 15.

Fairly big in size, the two sunspot groups cover almost two-thousandths of the solar hemisphere, a dozen times the surface area of the earth. Their length is 400,000 kilometres at its greatest.

One of the sunspot groups, appearing from the eastern edge of the solar face, was observed on April 3 and the other on April 5. They were spotted to be expanding extraordinarily fast. Freque t bursts have occurred, with April 6 being the biggest. They interfere with radio communications on earth.

According to the current speed of the sunspot groups and the structure of their magnetic field, the observatory predicts that the stronger group of the two has passed its prime and the other is still in its active stage.

Sunspot activity has about an 11-year cycle. The period from August, 1979 to February, 1981, the peak year of the solar activity, has been internationally acclaimed for solar study. More flares and sunspots will be observed in this period. Chinese astronomers are making use of this opportunity to conduct a series of studies.

Sunspot Activity Hypothesis Challenged

OW160232 Beijing XINHUA in English 0210 GMT 16 Apr 80 OW

[Text] Beijing, April 16 (XINHUA)--More than 300 scientists and historians who researched tens of thousands of old diaries and local records have challenged an American scholar's hypothesis that sunspot activity ceased for 70 years, from 1645 to 1715.

The hypothesis, put forward in 1976 by John Eddy, is the "Maunder Minimum" theory, pioneered in the last century by E. W. Maunder and Gustav Sporer.

The British newspaper, THE TIMES, recently carried a story which recorded the comments of Dr. Christopher Cullen, a Cambridge University researcher of Oriental science history, who had read a paper written by two Chinese astronomers which mentioned records of sunspots visible with the naked eye during the "Maunder" period.

According to THE TIMES, Dr. Cullen commented that more historical delving was needed to establish the reliability of the old Chinese records.

The 300 Chinese scientists and historians across the nation worked with the head of the Chinese Academy of Sciences, the Ministry of Education and the State Administrative Bureau of Museums and Archaeological Data.

They researched in three years more than 8,000 collections of old private and public records, as well as dynastic histories dating from antiquity up

to 1911, when the Qing Dynasty ended. The old records, totalling about 150,000 volumes, came from many counties in the provinces of Jiangsu, Henan, Shanxi, Shandong, Anhui, Zhejiang, Guangxi, Fujian, Guangdong and Hebei.

The scientists purpose was to make a general survey of ancient astronomical records. Coincidentally, they discovered 46 reports of major sunspot activity in the 17th century and 13 in the "Maunder" period identified by John Eddy. According to records of Anxi County in Fujian Province, for instance, major sunspots were observed on May 7, 1663 during the reign of Emperor Kangxi of Qing Dynasty.

They worked out a chart based on ancient Chinese astronomical observations recording sunspots, solar and lunar eclipses, comets, new stars and meteorites. They also compiled two huge volumes--"Historical Records in Astronomy" and "An Index of Chinese Local Notes".

Ting Youji, Luo Baorong and Feng Yongming of the Yunnan observatory and Zou Yixin of the Beijing observatory wrote papers in 1978 confirming the 11-year, 60-year and 250-year cycle of sunspot activity based on their research of old records. They concluded that Eddy's hypothesis was based on insufficient date.

Xu Zhentao of the Nanjing Purple Mountain observatory and Jiang Yaotiao of Nanjing University, a husband-and-wife partnership, whose paper caught the attention of Dr. Christopher Cullen in Britain, also confirmed in 1979 that sunspot activity followed the 11-year cycle during the "Maunder" period.

CSO: 4008

PHOTOGRAPHS REVEAL DETAILS OF TOKAMAK EXPERIMENTAL FACILITY

Beijing XIANDAIHUA [MODERNIZATION] in Chinese Vol 2 No 2, 16 Feb 80 back cover

[Photographs and captions]

Fig. 1. A portion of the longitudinal field coil and the vacuum chamber being assembled for China's first TOKAMAK facility.

Fig. 2. China's first TOKAMAK controlled thermonuclear reaction experimental facility (No. 6) at the Physics Institute, Chinese Academy of Sciences (photograph shows exterior of facility).

MICROWAVE SENSING TEMPERATURE RETRIEVAL DISCUSSED

Beijing DAQI KEXUE in Chinese Vol 3, No 3, Sep 79 pp 270-277

[Article by Zhao Bolin [6392 2672 2651], Peking University: "Problems of Retrieval in Remote Sensing of Atmospheric Temperature Stratification"]

[Text] Introduction

Retrieval in the remote sensing of atmospheric stratification requires solution of a type 1 Fredholm integral equation. In order to obtain a satisfactory result, a thorough physical analysis must be made of the problem to be solved, providing the constraints for the equations to be solved, and thus leading to an effective solution. This article discusses problems of inversion in microwave remote sensing from the ground. We first analyze the atmospheric noise which is the basis for remote sensing, then discuss inversion methods in the remote sensing of atmospheric temperature stratification, along with actual results and problems.

2. Radiation Transfer Formulas

In the atmospheric absorption spectrum, oxygen has strong absorption in the vicinity of 5 mm; in addition to absorption by the oxygen molecule, this band also contains weak continuous spectrum absorption by water. Oxygen is uniformly mixed in the lower atmosphere and its proportion in the air does not vary. Owing to strong absorption by oxygen and its unvarying proportion in air, temperature factors stand out in the radiation. When microwave radiation is used in remote sensing of atmospheric temperature stratification, the idea becomes reality.

The radiation transfer function for clear-weather horizontal atmospheric stratification is

$$T_s(\nu) = T_{\infty} e^{-\int_0^{\infty} \alpha \sec\theta\, dz} + \int_0^{\infty} T(z)\alpha e^{-\int_0^{z} \alpha \sec\theta\, dz} \sec\theta\, dz \qquad (1)$$

Here, $T_b(\nu)$ is the brightness temperature received at the earth's surface, ν is the frequency, α is the absorption coefficient, θ is the zenith angle, T(z) is the temperature stratification, z is the altitude, and T is the brightness temperature of outer space, equal to 3° K. Since the first term can be excluded as a known value, the inversion problem for equation (1) focuses on the second term of the right side of the equation. Thus

$$T_b(\nu) = \int_0^\infty T(z)\alpha e^{-\int_0^z \alpha \sec\theta dz} \sec\theta dz \qquad (2)$$

Using the pressure-altitude formula

$$p = p_0 e^{-\int_0^z \frac{g}{RT} dz}$$

(where g is the gravitational constant, R is the atmospheric gas constant, and p and p_0 are the gas pressure and the pressure at ground level respectively), equation (2) can be converted from altitude coordinates to gas-pressure coordinates:

$$T_b(\nu) = -\int_0^{p_0} T(z)\alpha e^{\int_p^{p_0} \alpha \sec\theta \frac{\partial z}{\partial p} dp} \sec\theta \frac{\partial z}{\partial p} dp \qquad (3)$$

The left side of equations (2) and (3) is the observed value, while T(z) on the right side is the value to be retrieved;

$$W = \alpha e^{-\int_0^z \alpha \sec\theta dz} \sec\theta \Delta z = -\alpha e^{\int_p^{p_0} \alpha \sec\theta \frac{\partial z}{\partial p} dp} \sec\theta \frac{\partial z}{\partial p} \Delta p = W_0 \Delta p$$

is the kernel of the inversion equation, and

$$W_0 = -\alpha e^{\int_p^{p_0} \alpha \sec\theta \frac{\partial z}{\partial p} dp} \sec\theta \frac{\partial z}{\partial p}$$

is the kernel when $\Delta p = 1$ mbar. This is a type 1 Fredholm integral equation, whose solution entails three problems:

1. Instability of the solution. The equation tends to magnify cumulatively the observational errors so that the relative importance of errors in the solution increases, rendering the solution unusable. Accordingly when a solution is being sought the input data and output results are smoothed to filter out high-frequency fluctuations. The maximum probability method and optimal fit method are used for selection purposes to decrease error interference.

2. Nonuniqueness of the solution. Equations (2) and (3) are solved by seeking a single solution out of a multiplicity, so that the solutions are not unique but multiple.

3. Nonlinearity of the kernel. The kernel W contains a complex relationship of the temperature T to be retrieved, and its nonlinearity makes the attempt to find a solution difficult. Linearization of the unique solution and the kernel requires an analysis of the physical nature of the problem, so as to derive constraints from it. Below we give an analysis of the character of the 5-mm band oxygen molecule radiation and the radiation formula based on atmospheric soundings made in the Peking region in 1964-1969 and 1970.

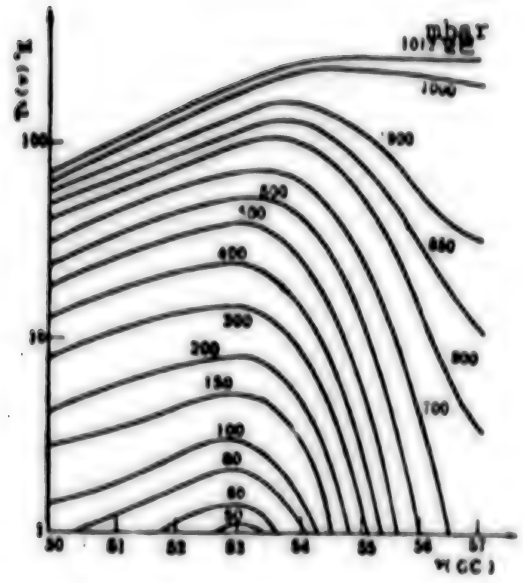

Fig. 1. Contribution of the atmosphere to the ground-level brightness temperature $T(\nu)$ above various isobaric surface altitudes.

1. The changes in temperature stratification are relatively small, and the mean square deviation is very small in comparison with the values themselves. Solutions may not deviate greatly from average values. At the same time, the average value is a good starting value.

2. The atmosphere acts as a barrier to downward penetration of upper-atmosphere radiation. Taking 53 GC, at which the upper atmosphere radiation is a maximum, as an example, above 300 mbar the brightness of radiation penetrating the atmosphere to the earth is only 10-20° K, equal to or less than a tenth of the total brightness; if so small a signal is used to analyze atmospheric temperature changes above 300 mbar, the error will inevitably be very large. In terms of information content, the lower the altitude of the temperature determination the more correct it is, and error accumulates with altitude.

3. The variation of the kernel function and the weighting function with frequency and angle are shown in Figs. 2 and 3. The weighting function drops off as altitude increases, with the decay being quicker as the frequency increases and the angle decreases. A low elevation angle and high frequency can reveal lower-atmosphere temperature stratification, while a high elevation angle and low frequency can reveal upper atmosphere stratification. The variation of the weighting function with temperature is very small, with every 1° change leading to a change of a few thousandths in the kernel function; accordingly it may be used as the iteration kernel. But the change cannot be ignored. For 53-GC vertical observations, for example, the calculation results are as in Fig. 4. In the lower atmosphere its

variation is analogous to that of the temperature change rate, and above 500 mbar it can even be greater than the temperature change rate, which introduces an error into the results of iterated high-altitude temperature stratification calculations.

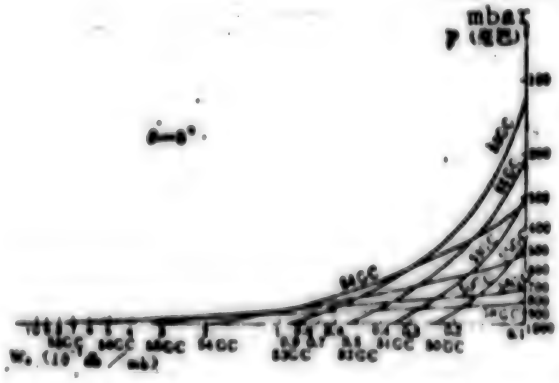

Fig. 2. Altitude distribution of the weighting factor at different frequencies ($\theta = 0°$).

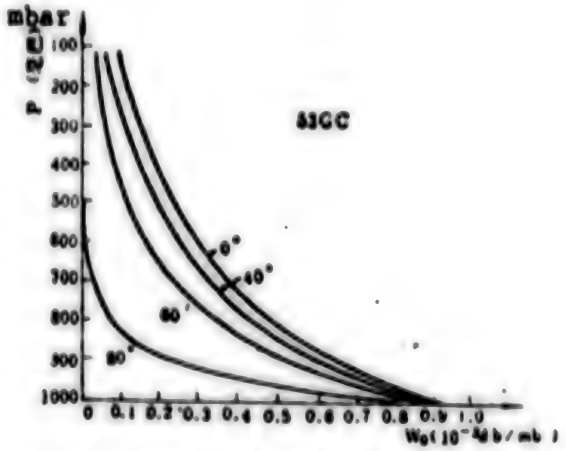

Fig. 3. Altitude distribution of the weighting factor at different angles (53 GC).

Equation 2 can be separated into the following forms

$$T_b(\nu) = T_0 + \int_0^{\infty} \frac{\partial T}{\partial z} e^{-\int_0^z \alpha \sec\theta\, dz} dz \qquad (4)$$

or

$$T_b(\nu) = T_0 - \int_0^{p_0} \frac{\partial T}{\partial z} e^{\int_p^{p_0} \alpha \sec\theta \frac{\partial z}{\partial p} dp} \frac{\partial z}{\partial p} dp \qquad (5)$$

Here T_0 is the ground-level temperature. The retrieved value in equations (4) and (5) is $\partial T/\partial z$.

$$W^* = e^{-\int_0^z \alpha \sec\theta\, dz} \Delta Z = -e^{\int_p^{p_0} \alpha \sec\theta \frac{\partial z}{\partial p} dp} \frac{\partial z}{\partial p} \Delta p = W_0^* \Delta p,$$

is the kernel of the inversion equation, and

$$W_0^* = -e^{\int_p^{p_0} \alpha \sec\theta \frac{\partial z}{\partial p}} \frac{\partial z}{\partial p}$$

is the kernel at $\Delta p = 1$ mbar. The kernel W_0^* decreases more slowly than W_0 as altitude increases. W^* also slowly levels off with temperature. Using survey data from the Peking region made at 0700 on 11-25 July 1970, and taking 53-GC vertical observations as an example, the rate of change of the kernel equation is

(where σ_T is the standard deviation of the temperature variation) and the temperature lapse rate σ_γ/γ (where σ_γ is the standard deviation of the temperature lapse rate and $\gamma = -\partial T/\partial z$) are compared, the rate of change of the kernel equation is an order of magnitude smaller than the rate of change of the temperature lapse rate

$$\left(\frac{\overline{\Delta W'^*}}{W^*} = 0.017, \frac{\sigma_\gamma}{\gamma} = 0.30\right)$$

so that the kernel equation W^* can be used as an iteration kernel.

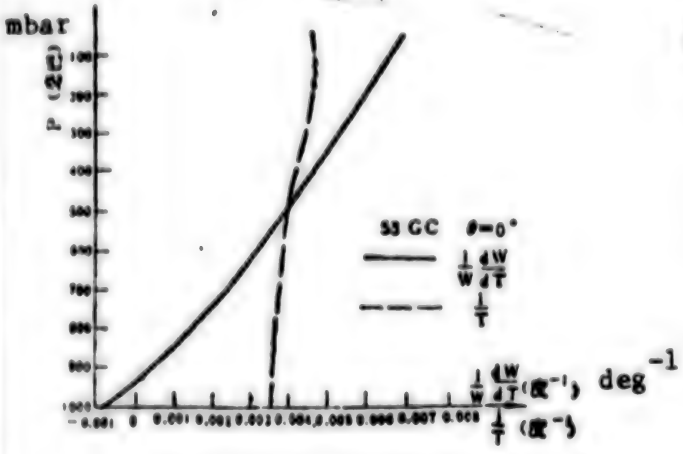

Fig. 4. Comparison of the rate of change of the weighting function with temperature with the rate of change of temperature (53 GC).

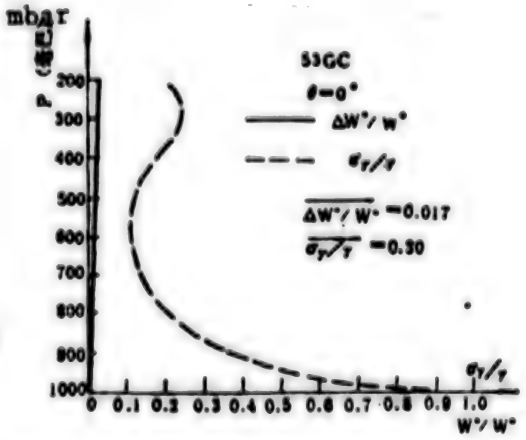

Fig. 5. Comparison of the rate of change of the weighting function with temperature with the rate of change of temperature (53 GC) [as published].

3. Retrieval Method

Previous atmospheric remote sensing methods have been numerous, including a combination of linear functions, an empirical orthogonal function scanning method, a least-squares control method, a smoothing method, an optimal extrapolation method, an estimation theory method, a statistical regression method, an artificial kernel equation method and an iteration method. Comparing these existing methods, the advantage of the iteration method is that it can express anomalous changes, is not limited by historical data and is easy to use. The temperature resulting from successive iterations converges with the brightness temperature, so that we can determine the temperature stratification distribution. We mainly use the iteration method to retrieve the atmospheric temperature distribution; we have a series of observational values for the brightness temperature T_{bi}, which we use to determine the initial value of the temperature stratification $T^{(0)}(z)$, which is substituted into equation (2), yielding

$$T_{bi}^{(0)}{}_{sat} = \int_0^\infty T^{(0)}(z)\alpha^{(0)} \sec\theta_i e^{-\int_0^z \alpha^{(0)} \sec\theta_i dz} dz \tag{6}$$

Note that the observed value of T_{bi} should be

$$T_{bi_{obs}} = \int_0^\infty T(z)\alpha \sec\theta_i e^{-\int_0^z \alpha \sec\theta_i dz} dz \tag{7}$$

From the discussion in section 2 we know that the kernel equation in (2) is not a sensitive indicator of temperature change. From equations (6) and (7)

$$T_{bi_{obs}} - T_{bi}^{(0)}{}_{sat} = \Delta T_i^{(0)}\left[1 - e^{-\int_0^\infty \alpha^{(0)} \sec\theta_i dz}\right] \tag{8}$$

or

$$\Delta T_i^{(0)} = \frac{T_{bi_{obs}} - T_{bi}^{(0)}{}_{sat}}{1 - \exp\left(-\int_0^\infty \alpha^{(0)} \sec\theta_i dz\right)} \tag{9}$$

and from equation (9) we have

$$\Delta T^{(0)}(z_j) = \frac{\sum_{i=1}^{m} W_{ij}^{(0)} \Delta T_i^{(0)}}{\sum_{i=1}^{m} W_{ij}^{(0)}} \tag{10}$$

and thus

$$T^{(1)}(z_j) = T^{(0)}(z_j) + \Delta T^{(0)}(z_j) \tag{11}$$

We then use $T^{(1)}(z)$ and iterate until convergence. On the n-th time through,

$$T_{bi}^{(n)}{}_{sat} = \int_0^\infty T^{(n)}(z)\alpha^{(n)} \sec\theta_i e^{-\int_0^z \alpha^{(n)} \sec\theta_i dz} dz \tag{12}$$

$$\Delta T_i^{(n)} = \frac{T_{bi_{obs}} - T_{bi}^{(n)}{}_{sat}}{1 - \exp\left(-\int_0^\infty \alpha^{(n)} \sec\theta_i dz\right)} \tag{13}$$

$$\Delta T^{(n)}(z_j) = \frac{\sum_{i=1}^{m} W_{ij}^{(n)} \Delta T_i^{(n)}}{\sum_{i=1}^{m} W_{ij}^{(n)}} \tag{14}$$

$$T^{(n+1)}(z_j) = T^{(n)}(z_j) + \Delta T^{(n)}(z_j) \tag{15}$$

Here

$$W_{ij}^{(n)} = \alpha^{(n)} \sec\theta_i e^{-\int_0^{z_j} \alpha^{(n)} \sec\theta_i dz} \Delta z_j^{(n)}$$

and iteration continues until $|T_{bi}^{(n+1)}{}_{sat} - T_{bi}^{(n)}{}_{sat}| < \delta$,

where δ is generally taken as 0.05-0.15° C.

Similarly we can use $\partial T/\partial z$ from equation (4) as the variable and iterate it. In the n-th iteration, using $T^{(n)}(z)$ as the initial value, we have

$$T_i^{(n)} = T_0 + \int_0^{\infty} \left(\frac{\partial T}{\partial z}\right)^{(n)} e^{-\int_0^z \sigma^{(n)} \sec\theta_i dz} dz \tag{16}$$

$$\Delta\left(\frac{\partial T}{\partial z}\right)_i^{(n)} = \frac{T_{i\text{测}} - T_i^{(n)}}{\int_0^{\infty} e^{-\int_0^z \sigma^{(n)} \sec\theta_i dz} dz} \tag{17}$$

$$\Delta\left(\frac{\partial T}{\partial z}\right)_j^{(n)} = \frac{\sum_{i=1}^{m} \Delta\left(\frac{\partial T}{\partial z}\right)_i^{(n)} W_{ij}^{*(n)}}{\sum_{i=1}^{m} W_{ij}^{*(n)}} \tag{18}$$

$$\left(\frac{\partial T}{\partial z}\right)^{(n+1)} = \left(\frac{\partial T}{\partial z}\right)^{(n)} + \Delta\left(\frac{\partial T}{\partial z}\right)_j^{(n)} \tag{19}$$

$$T^{(n+1)}(z) = T_0 + \int_0^z \left(\frac{\partial T}{\partial z}\right)^{(n+1)} dz \tag{20}$$

Here

$$W_{ij}^{*(n)} = e^{-\int_0^{z_j} \sigma^{(n)} \sec\theta_i dz} \Delta z_j^{(n)}.$$

Iteration proceeds until

$$|T_{i\text{测}}^{(n+1)} - T_{i\text{测}}^{(n)}| < \delta$$

We made simulation calculations on the basis of average measurements for Peking for 1964-1969. In this calculation, following references 3 and 4 [not reproduced] we took account only of oxygen absorption in order to investigate the speed of convergence of the iteration. At 50-60 GC, we selected 18 frequencies and used a frequency scan method to perform the inversion. The initial value was a standard large-scale model:

$$\begin{cases} T(z) = T_0 - \gamma z & z \leqslant 11.0\text{ km} \\ T(z) = \text{常数} & z \geqslant 11.0\text{ km} \end{cases} \qquad \gamma = 0.65\text{℃}/100\text{ m} \tag{21}$$

After threefold iteration using the inversion method of equations (7)-(11) and (16)-(19), the results shown in Figs. 6 and 7 were obtained. From these figures it can be seen that iteration convergence is very rapid and the final error is not very large. The values from the two inversion methods do not differ greatly.

Here we used data from remote sensing of atmospheric temperature stratification taken by Peking University, the Shanghai Meteorological Instruments Plant and the Peking Plant No 768 from ground level with a 52.9-GC microwave radiometer to illustrate the results of retrieval by the iteration method. The inversion method used was that of equations (7)-(11). Ground-level humudity readings and predicted distributions from climatic data were used to predict the influence of water vapor, and it was taken as a known value in the equation. The results of observations by the

angular scan method are shown in Fig. 8. In temperature determination work, it can reveal lower-atmosphere temperature inversions, while upper-atmosphere convergence generally depends on the selection of the initial value. Because meteorological variations are continuous, if recent observational data are used as initial data the convergence will be better. Fig. 9. shows the error as a function of altitude. It can be seen from the figure that the error in microwave remote temperature sensing increases with altitude.

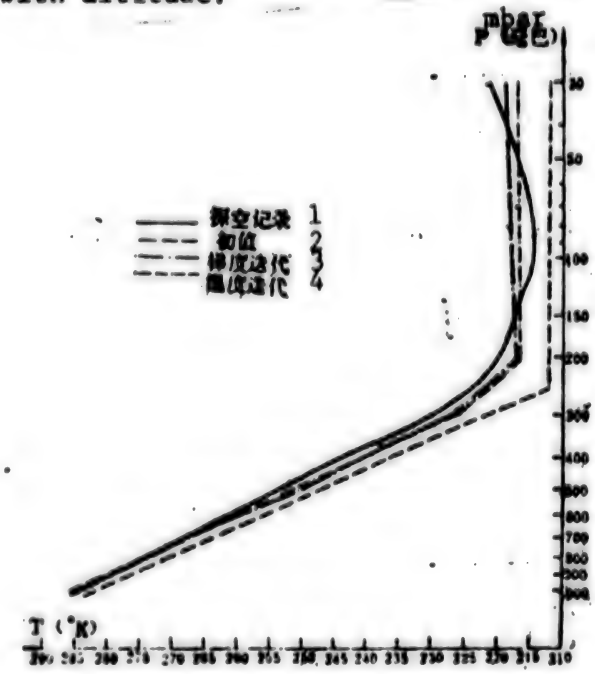

Fig. 6. Results of retrieval of temperature stratification at Peking by the frequency scan iteration method (threefold iteration).

Key: 1. Control data
2. Initial value
3. Gradient iteration
4. Temperature iteration

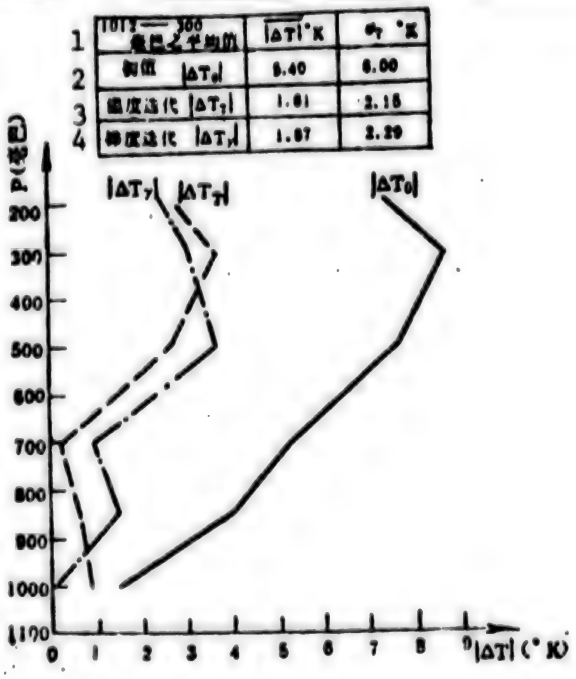

Fig. 7. Error of iteration retrieval (threefold iteration).

Key: 1. Average value for 1012-300 mbar
2. Initial value of $|\Delta T_0|$
3. Temperature iteration $|\Delta T_1|$
4. Gradient iteration $|\Delta T_2|$

4. Discussion

For correct ground-based remote sensing of atmospheric temperature stratification we must take into account the effect of humidity and cloud. Although both humidity and cloud cover are of small account in the 5-mm range, they cannot be ignored. When the 1.35-cm humidity determination band and the 8-mm cloud determination band are added, not only can the humidity and cloud moisture values be determined but the accuracy of temperature determination can be increased.

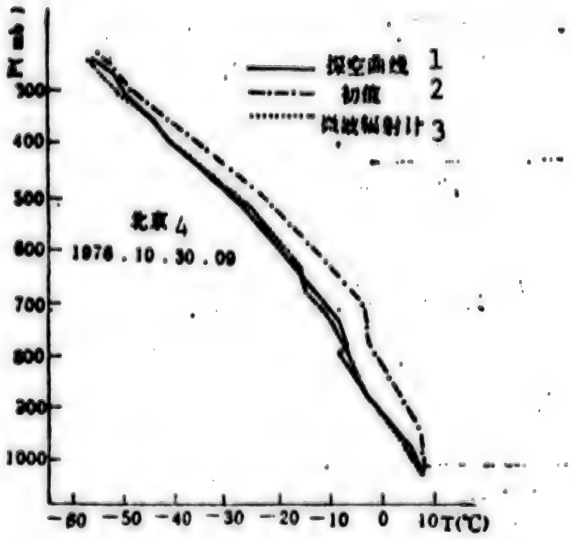

Fig. 8. An actual example of angular-scan microwave remote-sensing temperature determination (52.8 GC).

Key: 1. Curve from atmospheric soundings.
2. Initial value
3. Microwave radiometer
4. Peking

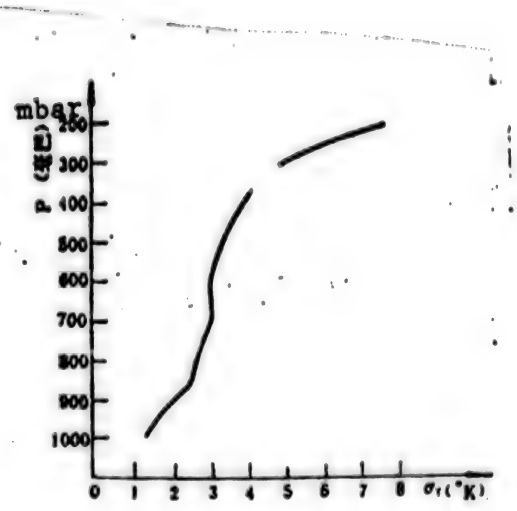

Fig. 9. Microwave remote-sensing temperature determination error at 52.8 GC, angular scan method, 33 tests in October-November 1976, Peking.

1. The effect of humidity. Using scanning method observations in the 1.35-cm band, the brightness temperature is as in equation (4)

$$T_b(\theta) = T_0 + \int_0^\infty \left(\frac{\partial T}{\partial z}\right) e^{-\int_0^z \alpha \sec\theta\, dz}\, dz \qquad (4)$$

The absorption coefficient α is equal to $\alpha_{O_2} + \alpha_{H_2O}$, where α_{O_2} is the absorption coefficient for oxygen and α_{H_2O} is the absorption coefficient for water. Moreover $\alpha_{H_2O} = Aq$, where q is the relative humidity and A is a temperature-pressure-humidity function, If we let

$$u = \int_0^z \alpha dz \qquad \text{and} \qquad \Delta u = \frac{\Delta q}{q} \int_0^z Aq dz,$$

then

$$\Delta T_b = -\int_0^\infty \left(\frac{\partial T}{\partial z}\right) \Delta u \sec\theta e^{-u\sec\theta}\, dz = -\frac{\Delta q}{q} \int_0^\infty \left(\frac{\partial T}{\partial z}\right) \sec\theta \left(\int_0^z Aq dz\right) e^{-u\sec\theta} dz \quad (22)$$

Using the result of the q-th iteration $q^{(n)}$, we obtain from equation (4)

$$T_{b1}^{(s)}{}_{u} = T_0 + \int_0^{\infty} \left(\frac{\partial T}{\partial z}\right) e^{-\int_0^z (\alpha_{O_2} + \Delta q^{(s)}) \sec\theta_i dz} dz \qquad (23)$$

so that

$$T_{b1m} - T_{b1u}^{(s)} = -\frac{q_1^{(s+1)} - q^{(s)}}{q^{(s)}} \int_0^{\infty} \left(\frac{\partial T}{\partial z}\right) e^{-\int_0^z (\alpha_{O_2} + \Delta q^{(s)}) \sec\theta_i dz} \times \sec\theta_i \left(\int_0^z \Delta q^{(s)} dz\right) dz \qquad (24)$$

and

$$q_1^{(s+1)} = q^{(s)}\left[1 - \frac{T_{b1m} - T_{b1u}^{(s)}}{S_1^{(s)}}\right] \qquad (25)$$

where

$$S_1^{(s)} = \int_0^{\infty} \left(\frac{\partial T}{\partial z}\right) e^{-\int_0^z (\alpha_{O_2} + \Delta q^{(s)}) \sec\theta_i dz} \times \sec\theta_i \left(\int_0^z \Delta q^{(s)} dz\right) dz.$$

and

$$q^{(s+1)} = \frac{\sum_{i=1}^{\bar{n}} q_i^{(s+1)} V_{ij}}{\sum_{i=1}^{\bar{n}} V_{ij}} \qquad (26)$$

where

$$V_{ij} = e^{-\int_0^{z_j} (\alpha_{O_2} + \Delta q^{(s)}) \sec\theta_i dz} \times \sec\theta_i \left(\frac{\partial T}{\partial z}\right) \Delta z_j.$$

Iteration is continued until

$$|T_{b1u}^{(s+1)} - T_{b1u}^{(s)}| < \delta$$

If we use 5-mm and 1.35-cm microwave radiometer remote sensing of temperature and humidity stratification and employ equations (7)-(15) and (23)-(26), successively iterating temperature and humidity until convergence, it is possible to retrieve the atmospheric temperature and humidity stratification. Reference 29 [not reproduced] carried out a simulation calculation with the result shown in Fig. 10. When the 5-mm and 1.35-cm bands are used in microwave sensing of atmospheric temperature and humidity stratification, more correct results can generally be obtained.

2. The effect of cloud. The effect of non-precipitation cloud cover in the 5-mm and 1.35-cm ranges is small, but cannot be ignored in remote sensing of atmospheric stratification (see Fig. 11). The influence of non-precipitation cloud layers is relatively large at frequencies below 53 GC, because in the high-frequency region atmospheric attenuation is large and the effect of cloud is blocked (see fig. 12). Because the effect of cloud in temperature sensing (5 mm) and humidity sensing (1.35 cm) shows up as a small quantity in the brightness temperature, 8-mm remote sensing can be used to determine the effect of cloud. Absorption by water vapor and its contribution to brightness is almost 3 times as great in the 1.35-cm range as in the 8-mm range; absorption by cloud and its contribution to brightness is 2 1/2 times as great in the 8-mm band

as in the 1.35-cm band. If sensing is done at 8 mm and 1.35 cm, the effect of atmospheric humidity and the quantity of moisture in the clouds can be taken into account; accordingly this can be used to correct 5-mm remote sensing figures on atmospheric temperature stratification for the effect of cloud. By using 8-mm, 1.35-cm and 5-mm sensing, it is possible to obtain data on atmospheric temperature, humidity, pressure and cloud moisture. Microwave remote sensing of atmospheric stratification has the advantage of being flexible and giving continuous data, and it is suitable for dissemination and use in lower-atmosphere surveys.

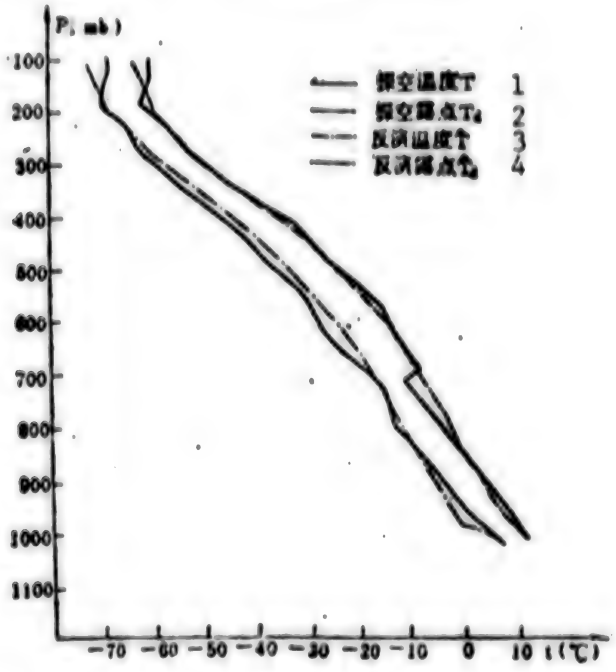

Fig. 10. Simulation calculation of atmospheric temperature and humidity stratification using microwave remote sensing at 5 mm and 1.35 cm.

Key: 1. Temperature T from soundings
2. Dewpoint T_d from soundings
3. Retrieved temperature T
4. Retrieved dewpoint T_d

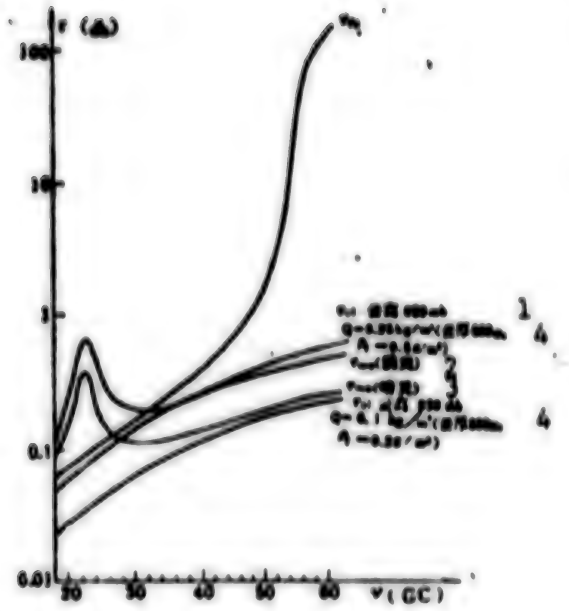

Fig. 11. Distribution of absorption by atmospheric oxygen, water vapor and cloud as a function of frequency.

Key: 1. Cloud height
2. Clear weather
3. Cloudy weather
4. Cloud thickness

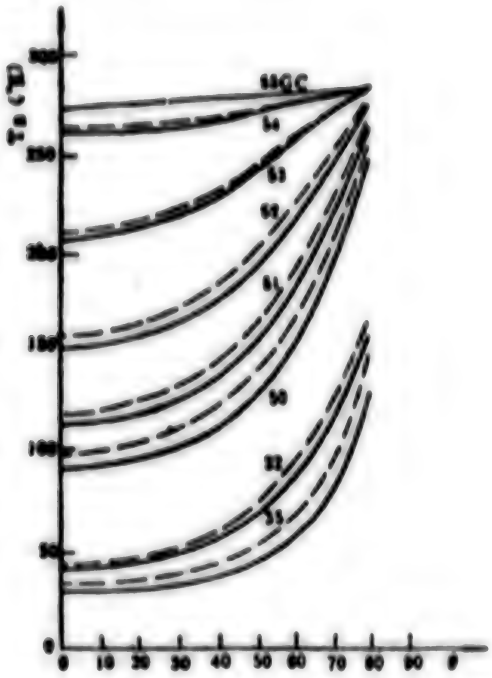

Fig. 12. Effect of cloud layers on brightness temperature (cloud height 850 mbar, thickness 500 meters, moisture content 0.2 g/m^3).

Key:

Solid line: effect of unsaturated cloud layer;
Broken line: effect of saturated cloud layer.

8480
CSO: 4008

AUTHOR: Theater Design Group, Zhejiang Provincial Industrial Design Institute

ORG: None

TITLE: "The Design of the Hangzhou Theater"

SOURCE: Beijing JIANZHU XUEBAO [ARCHITECTURAL JOURNAL] in Chinese No 1, Jan 80 pp 1-7, 56

TEXT OF ENGLISH ABSTRACT: The newly built Hangzhou theater has a seating capacity of 2,000 and a volume of some 10,000 cubic meters. The bell-shaped auditorium measures 31.5 x 36 meters with a balcony holding about 700 seats. The sidewalls are faced with fine-grained wooden slats; 144 boat-shaped diffusers made of mesh-reinforced cement are suspended from the ceiling. In the vestibule are two free-standing spiral staircases with curved landings supported by a tier of slender columns faced with white marble. The exterior wall surface consists mainly of large blue glass window areas and panels faced with white marble chips. The reverberation time in the auditorium is 1.5, 2.1 and 1.4 seconds at middle, low and high frequencies respectively (fully occupied). The sound field distribution difference for middle frequencies is less than 5 bD for low frequencies and 4 dB for high frequencies. The diffusion directionality value is above 80% and the articulation of natural sound over 85%.

AUTHORS: YE Sujuan [1673 4930 1221]
YE Hengjian [1673 1854 0256]
CUI Shunsheng [1508 7311 3932]
CAO Xiaozhen [2580 1321 2182]
TANG Baoheng [0781 5508 0077]
SHEN Jihuang [3084 3444 7806]

ORG: Ye, Ye, Cui and Cao of Chinese Institute of Construction Science; Tang and Shen of Zhejiang Provincial Industrial Design Institute.

TITLE: "Acoustic Design of the Hangzhou Theater"

SOURCE: Beijing JIANZHU XUEBAO [ARCHITECTURAL JOURNAL] in Chinese No 1, Jan 80 pp 8-12

ABSTRACT: Because the Hnagzhou theater was designed primarily for musical performances, while also intended to be usable for other purposes, a relatively long reverberation time was desired. In addition, it was desired to assure adequate early reflected sound in the guest boxes at the front of the theater. The latter problem was solved by angling the walls and ceiling directly outside the stage opening so as to reflect the sound toward the boxes. Irregularly shaped particle-board reflectors were placed at four

[Continuation of JIANZHU XUEBAO in Chinese No 1, Jan 80 pp 8-12]

locations on the side walls, 3.65 and 8.60 meters above the standard source height to improve reflective coverage of the rest of the hall. The side supports of the proscenium arch were angled forward at 23° to improve reflection to the guest boxes. Measurements of reverberation time showed figures of 2.1, 1.5 and 1.4 seconds at low, middle and high frequencies. Sound clarity with both a single speaker and music was measured and found to be satisfactory. In most of the auditorium, the sound variation with direction was no lower than 80%. The sound distribution was satisfactory, being a maximum drop of 5 dB at 500 Hz and 4 dB at 2,000 Hz. Initial testing was done on a 1/10 scale model.

AUTHOR: ZHANG Jinqiu [1728 6930 4428]

ORG: NONE

TITLE: "A Memorial to Abeno Nakamaro"

SOURCE: Beijing JIANZHU XUEBAO [ARCHITECTURAL JOURNAL] in Chinese No 1, Jan 80 pp 13-14

TEXT OF ENGLISH ABSTRACT: Abeno Nakamaro, known in China as Chao Heng, was born in Nara, Japan, and came to China in 717. He became an officer under the Tang Dynasty, serving for 50 years. Excelling in Chinese poetry, he was a friend of the Tang poets Li Bo and Wang Wei. He died in Changan in 770. The memorial, completed in summer 1979 in Zingqing Park, Xian, is made of stone and imitates the column form of Tang architecture. Its shaft is square with entasis derived from the Chinese traditional architectural style and topped with a pyramidal roof. The memorial stands on a 6 meter square platform. The inscriptions relate Abeno's biography and present one of his poems and a poem composed for him by Li Bo. The surroundings are landscaped with evergreen pines, cypresses and cherry trees.

AUTHOR: YU Shengfang [0205 4939 2455]

ORG: None

TITLE: "A Masterpiece of Ancient Chinese City Planning"

SOURCE: Beijing JIANZHU XUEBAO [ARCHITECTURAL JOURNAL] in Chinese No 1, Jan 80 pp 15-20

TEXT OF ENGLISH ABSTRACT: The city of Suzhou was subjected to city planning during the Song Dynasty. In 1229 the governor of the district engraved a plan for the city with considerable accuracy on a large tablet measuring roughly 6'6" x 4'5". This engraving shows the exact details of the layout of the city, including the city wall with its bastions, roads, canals, bridges, walled enclosures of important groups of buildings and the surrounding lakes and hills in the suburbs. It is an extremely valuable historical document for city planning and construction. Analysis of the planning indicates that: 1. use was made of navigable rivers and of building materials available in the suburban hills; 2. the traffic system included both roads and canals, with the canal system practically duplicating the road system and being spanned by about 300 bridges; 3. the roads in the city were in a north-south, east-west rectangular grid. Many buildings were set up along the canals, and the most important enclosures were surrounded by water; 4. architectural elements were skillfully disposed to form a varied and intriguing spatial composition.

AUTHOR: AI Dingzeng

ORG: None

TITLE: "Some Wrong Trends in Architectural Creation"

SOURCE: Beijing JIANZHU XUEBAO [ARCHITECTURAL JOURNAL] in Chinese No 1, Jan 80 pp 21-22

ABSTRACT: In order to eliminate rigidity and semirigidity in architectural style, the following bad trends should be opposed: 1. Archaism and formalism. Buildings should reflect both the changes in society and the development of materials technology. 2. Hesitation to depart from old practices and a stereotyped approach. This stems from fear of offending government officials and develops into fear of innovation. It also includes unjustified rejection of progressive Western trends such as the stress on the human element in architecture and the recognition that functional is beautiful. 3. Ultraleftist influences. These are relics from Lin Biao and the "gang of four." Excessive use of political slogans, quotations, red flags and portraits are a major manifestation. Surface political manifestations should not take the place of architectural creativity.

AUTHORS: ZHONG Xunzheng [6988 6064 2973]
XI Shuxiang [1153 2885 4382]

ORG: None

TITLE: "Letting 'A Hundred Flowers Bloom and a Hundred Schools Contend' in Architecture"

SOURCE: Beijing JIANZHU XUEBAO [ARCHITECTURAL JOURNAL] in Chinese No 1, Jan 80 pp 23, 37

ABSTRACT: The contending of different architectural schools has experienced some difficulties in China, since lacking the criticism of the masses the main thing that has resulted has been "forbidden areas," particularly following the 1954 criticism of the return to old styles. Since the defeat of the "gang of four" both the attitude toward design and the feeling about foreign ideas and approaches have become somewhat freer. In Europe before the First World War, a contention of schools produced bold new architectural approaches. In Peking during the 50's, the Heping [0735 1627] Hotel, which was a new departure, was criticised as bourgeois, "inhuman" and formalistic, but it now stands vindicated against skyscrapers and Soviet-style buildings. Chinese architecture in the 30's was monotonous because of absence of contending schools. Recent work in Canton is breaking new ground.

AUTHOR: CAO Qinghan [2580 1987 3211]

ORG: None

TITLE: "Criticism of 'Station and Torch'"

SOURCE: Beijing JIANZHU XUEBAO [ARCHITECTURAL JOURNAL] in Chinese No 1, Jan 80 p 24

ABSTRACT: The Changsha Railway Station and its symbolic torch have come in for considerable criticism. The author replies to HU Dunchang's [5170 2415 1603] article "Station and Torch" (JIANZHU XUEBAO No 3, 1979). He agrees with the article to the extent that a building must first be functional but adds that after this requirement is satisfied more may still be done. Buildings may be functional and at the same time artistic and evocative in a way that is in keeping with function; the design of Roman temples, Renaissance churches and later theaters is cited. But evocatively symbolic elements should not be so complex that they need a guidebook for their decipherment.

AUTHOR: ZHU Yuqing [2612 3558 7230]

ORG: None

TITLE: "Comment on the Monument Commemorating the August 1 Nanchang Uprising"

SOURCE: Beijing JIANZHU XUEBAO [ARCHITECTURAL JOURNAL] in Chinese No 1, Jan 80 p 25

ABSTRACT: Of the various monuments to heroic feats of the Civil War, some are more successful than others. The monyment commemorating the August 1 Nanchang Uprising, described in JIANZHU XUEBAO No 3, 1979, although it shows some inventive touches, is basically derivative from earlier monumental style and does not show an insiration worthy of the deeds which it commemorates. The inscription is overpowering and discordant, and not in keeping wich Chairman Hua's modesty and humility. Moreover the design as a whole is not well suited to its surroundings, but fits into them incongruously.

AUTHOR: YANG Yun

ORG: China Construction Science Institute

TITLE: "Some Reflections on Current Trends in Western Architecture"

SOURCE: Beijing JIANZHU XUEBAO [ARCHITECTURAL JOURNAL] in Chinese No 1, Jan 80 pp 26-34

TEXT OF ENGLISH ABSTRACT: This article briefly described and analyzes the new trends in Western contemporary architecture, especially the main features of "postmodernism." Connecting these trends with the problems often encountered by Chinese architects in their practice, the writer puts forward his own view points concerning the orientation of architectural design. He maintains that (1) objective physical and technological conditions are still the basis of architectural creation; (2) the architectural form can have an influence upon people's ideology and feelings, and the architectural image can be created to a certain extent according to designers' intentions; (3) it is necessary to assimilate the useful experience from the development of the modern Western architectural movement as a whole, especially the experinece of industrialization.

AUTHORS: ZHOU Huilin [0719 1979 2651]
LU Zhauquan [0712 4801 2164]

ORG: None

TITLE: "A Semi-Maisonette Housing Design Project"

SOURCE: Beijing JIANZHU XUEBAO [ARCHITECTURAL JOURNAL] in Chinese No 1, Jan 80 pp 35-37

ABSTRACT: An apartment complex layout is described in which the daily living space is laid out on one side of the building with a relatively large area and high ceilings, while auxiliary space such as kitchens is laid out on the other side of the building with relatively small floor area and low ceilings. Three variants are nested together: one variant has two small rooms split upwards and downwards from the main living space, while the other two variants have single auxiliary rooms either on the same level or slightly above; the result is that five main living areas and seven auxiliary rooms can be stacked in an apartment building 15.75 meters high. Layouts of the three variants are given. The floor space ranges from 24.67 to 41.95 square meters.

AUTHOR: ZHOU Buyi [0719 0592 7328]

ORG: Department of Construction Engineering, Qinghua University

TITLE: "Comments on Some Famous Buildings of the Seventies in Europe and America"

SOURCE: Beijing JIANZHU XUEBAO [ARCHITECTURAL JOURNAL] in Chinese No 1, Jan 80 pp 43-56

ABSTRACT: The following buildings are described and commented on: 1. the Bonaventure Hotel in Los Angeles (John Portman, designer); 2. the National Cultural Center in Paris (Rengo Piano and Richard Rogers); 3. the English National Theater in London (Denys Lasdun); 4. the East Wing of the National Gallery of Art in Washington (Bei Yueming); 5. the Johns Manville Building, World Sales Center (TAC).

AUTHORS: DU Xibin [2659 1585 2430]
CHEN Huiling [7115 1920 3781]
ZHANG Xiangxuan [1728 4382 5503]
GAO Xizhou [7559 6932 0046]

ORG: None

TITLE: "Industrial Buildings in the Federal Republic of Germany"

SOURCE: Beijing JIANZHU XUEBAO [ARCHITECTURAL JOURNAL] in Chinese No 1, Jan 80 pp 57-63

ABSTRACT: The following topics are discussed: reinforced and prestressed concrete construction, including T-shaped and V-shaped constructions for single-story factory roofs, and double-T and sawtooth structures, as well as types of framing for multistory factories; new reinforced concrete thin panels with insulating and water-resistant properties, pressurized thin panels and rock wool-cement tiles; interior wall panels and methods of joining and decorating them; and types of skylighting and sidewall window construction in single-story factory buildings.

AUTHOR: None

ORG: None

TITLE: See below

SOURCE: Beijing JIANZHU XUEBAO [ARCHITECTURAL JOURNAL] in Chinese No 1, Jan 80 inside and outside front covers

ABSTRACT: Outside front cover: Aerial view of coal classification plant, Jiangzhuang [5592 8369] al Mine, Tengnan [3326 0589] Mining District, Shandong (painting).

Inside front cover: Map of Suzhou during the Song Dynasty.

Inside back cover: Photographs of a U. S. luxury hotel, French National Cultural Center.

Outside back cover: Islamabad Sports Complex, Pakistan; Guilin Railway Station.

8480
CSO: 4009

DUALITY RELATION AND STATE ESTIMATION IN SYSTEMS WITH UNCERTAINTY

Beijing ZIDONGHUA XUEBAO [ACTA AUTOMATICA SINICA; JOURNAL OF AUTOMATION] in Chinese Vol 5 No 1, 1979 p 5

Han Jingqing [7281 0079 3237], Institute of mathematics, Academia Sinica

[Abstract] The present paper discusses the problem of state estimation for the following system

$$\begin{cases} \dot{x} = A(t)\,x + B_1(t)\,u(t) + B_2(t)\,w \\ y = C(t)\,x + D_1(t)\,u(t) + D_2(t)\,w \end{cases}$$

where u (t) is the known input vector and W the uncertain vector. Assume that W is a function of t, for which we know its range of variation only, but we do not know its concrete realization. The problem is that how to estimate the state variables x (T) on the base of observation values y (t), $0 \leqslant t \leqslant T$. The duality relation established in [1] is used to solve the problem of the min-max estimation. The min-max state estimation under the limitation of quadratic constraints coincides exactly with the Kalman filter. The method used here is much simpler than that of [4].

CSO: 4020

A MATHEMATICAL MODEL OF COMPUTER-CONTROLLED CREEP-TESTING FURNACES

Beijing ZIDONGHUA XUEBAO [ACTA AUTOMATICA SINICA; JOURNAL OF AUTOMATION] in Chinese Vol 5 No 1, 1979 p 14

Wang Jiasheng [3769 1367 5116], Institute of Teachers, Shanghai;
Cheng Yufan [6774 3022 5603], University of Teachers, Shanghai

[Abstract] An example of utilizing the modern control theory is discussed in this paper. The controlled object is an electric furnace with two independent heating windings. Two thermocupls are used to measure the furnace temperature at two different points. The accuracy of controlling the temperatures of the upper and lower portion of the furnace is better than $\pm 2°C$. The object is treated as a LQG system with two variables. The mathematical model consists of dynamic mathematical model, a Kalman filter, an optimum state feedback and the self adapting set point following computation.

This control system has been used in controlling more than seventy similar furnaces with a small process-control computer.

CSO: 4020

MULTI-FUNCTIONAL PSUEDORANDOM BINARY SEQUENCE CORRELATOR AND ON-LINE IDENTIFICATION OF CONTROL SYSTEMS OF COLD ROLLING MILLS

Beijing ZIDONGHUA XUEBAO [ACTA AUTOMATICA SINICA; JOURNAL OF AUTOMATION] in Chinese Vol 5 No 1, 1979 p 29

Li Bainan [2621 4101 0589], Zhong Yanjiong [6988 1693 3518], Peking Institute of Iron and Steel Technology]

[Abstract] This paper describes the design of pseudorandom binary sequence correlator based on the principles of on-line identification. An experimental procedure is suggested. Therefore a multi-periods inverse-repeat m sequence is synchronized with real time binomial weighted averaging in order to eliminate the effect of polynomial drift to the estimated impulse response. The system is prior excited by a periodic pseudorandom signal. It can eliminate the effects of nonstationary process. Two m sequence of inverse-repeat shifting 1/2 half-periods can be considered as independent sequence, which identify a multidimensional system. The experiments have proved the effectiveness of these methods which increases identification accuracy and enlarge the function of the equipment function. At last, this paper presents the on-line identification and the on-line regulation of control systems for cold rolling mills.

CSO: 4020

OPTICAL CHARACTER RECOGNITION SYSTEM (OCR)

Beijing ZIDONGHUA XUEBAO [ACTA AUTOMATICA SINICA; JOURNAL OF AUTOMATION] in Chinese Vol 5 No 1, 1979 p 38

Zhou Xin [6650 2450], Qian Luoqiu [6929 2867 7264], University of Futan, Shanghai

[Abstract] The Optical Character Recognition System of Futan 780 model has been developed for a special demand. The aim of the system is to recognize the alphabet and some special marks which have been machine-printed on certain document papers. The researching target of the system is that under the recognition speed of 100 characters per second both the substitution rate and reject rate approaches to 10^{-4} (including the black/red colour recognition substitution rate). Because of the lower case alphabet the system is to recognize and automatically continuously printing in the document-making process, the printing quality varies a great deal. So we are confronted with a difficult situation in the aspect of character recognizability.

[continuation of ZIDONGHUA XUEBAO Vol 5 No 1, 1979 p 38]

This paper will describe the developing process of the system and how to select the scheme. Basing on it, a two-stage recognition scheme with the combination of hardware and software will be set forth. Finally this paper will present the experimental results and the orientation of its improvement.

CSO: 4020

A NEW TYPE OF MICROWAVE THICKNESS METER

Beijing ZIDONGHUA XUEBAO [ACTA AUTOMATICA SINICA; JOURNAL OF AUTOMATION] in Chinese Vol 5 No 1, 1979 p 57

Xiao Zhonghan [5135 0022 3352], Chungking Institute of Industrial Automation Instruments

[Abstract] A new type of microwave thickness meter is described. The thickness is gaged fast and accurately by using a method of self-balancing microwave, bridge and metering argument of input reflection coefficient of a "equivalent short." In this paper, it's design, computation and experiment model were all outlined.

CSO: 4020

THE THEORY OF MAXIMUM MAGNETIZING CURRENT IN TRANSISTOR DC-DC CONVERTER

Beijing ZIDONGHUA XUEBAO [ACTA AUTOMATICA SINICA; JOURNAL OF AUTOMATION] in Chinese Vol 5 No 1, 1979 p 73

Sun Dinghao [1327 1357 3185], Zhu Demao [4281 1795 2021], Liao Jiongsheng [1675 4741 3932], Peking Institute of Control Engineering

[Abstract] In this paper, the transistor DC-DC converter as a whole is analyzed by the theory of oscillations.

Neglecting the effect of parasitic capacitance, the discontinuous vibration, in which there are two different jump phenomena, exists in the converter. The jump phenomenon I is particular to the converter; the jump phenomenon II is the same as that happens in the DC-AC inverter. The cause resulting in both jump phenomena is that the magnetizing current reaches the maximum under the existing state of the converter.

Theoretical prediction is consistent with experimental results.

CSO: 4020

ARTIFICIAL INTELLIGENCE

Beijing ZIDONGHUA XUEBAO [ACTA AUTOMATICA SINICA; JOURNAL OF AUTOMATION] in Chinese Vol 5 No 1, 1979 p 57

Li Jiazhi [2621 1367 3112], Institute of Psychology, Academia Sinica; Wang Yunjiu [3076 0061 0046], Institute of Bio-physics, Academia Sinica; Tu Xuyan [3205 1645 1750] and Guo Rongjiang [6753 2837 3068], Institute of Automation, Academia Sinica

[Abstract] Research developments of artificial intelligence in foreign countries were surveyed under five headings since its early beginnings up to the present time.

1. Brain and neural models. Studies related to brain and neural models were evaluated and their importance for the understanding of the nature of human and artificial intelligence was emphasized.

2. Thinking process simulation. The seking for heuristics from human intellectual activities has been stressed for the realization of artificial intelligence.

[continuation of ZIDONGHUA XUEBAO Vol 5 No 1, 1979 p 57]

3. Pattern recognition. Visual pattern recognition problems involving statistical and syntactic approaches as well as robot vision were specifically discussed.

4. Understanding natural language. A general outline was given for the development trends from the syntactic analysis in the late fifties to the memory models of semantic network and then to the conceptual dependence theory in the early seventies.

5. Intelligence robots. Description was made on the MIT, Stanford University and some of the Japanese robots.

Based upon the above review, the authors concluded with the opinion that the study of artificial intelligence should be regarded as an interdisciplinary science of intelligence, and outstanding achievements were anticipated from the joint efforts by scientists from different disciplines.

CSO: 4020

THE INVESTIGATION OF HANDWRITTEN CHARACTERS RECOGNITION METHODS

Beijing ZIDONGHUA XUEBAO [ACTA AUTOMATICA SINICA; JOURNAL OF AUTOMATION] in Chinese Vol 5 No 1, 1979 p 46

Dai Ruwei [0108 3067 3634], Hu Chiheng [5170 0796 1854] et al, Institute of Automation, Academia Sinica

[Abstract] One of the important application of handwritten characters recognition machine is to read postal codes in the automatic letter sorting. In this article, we shall briefly introduce a handwritten numeral recognition machine which is used for automatic letter sorting, and discuss the design of sequential recognition logics by means of results of grammatical inference of finite state grammar, as well as the idea of Fuzzy sets for information compression.

CSO: 4020

AUTHOR: LI Changhua [2621 2490 0553]

ORG: None

TITLE: "Three-Gorge Water Conservancy Headquarters--Number One Important Engineering of China's Four Modernisations"

SOURCE: Beijing KEXUE SHIYAN [SCIENTIFIC EXPERIMENT] in Chinese No 10 Oct 79 pp 1-3

ABSTRACT: From 1911 to 1949 there had been 7 floods in the Yangzi valley. The hydrological and meteorological reasons of these floods are discussed. Premier Zhou pointed out in 1958 following a personal inspection of the region that there is no way to control floods of the Yangzi without constructing a water conservancy headquarters in the Three-gorge. Since then, designs which include one of twenty largest dams in the world and the greatest hydroelectric generation system of the world have been formulated. The paper describes the various functions of the water conservancy project at the Three-gorge and the scale of this project. There is no mention of the expected date of completion, however. Under the leadership of HUA Guofeng, all technical problems of constructing the project can be resolved, the author simply promises.

AUTHOR: None

ORG: Special Subject Group for the Comprehensive Utilization of Panzhihua Ore Deposit

TITLE: "Comprehensive Utilization of Panzhihua Ore Deposit--Extracting Treasure From the Mine"

SOURCE: Beijing KEXUE SHIYAN [SCIENTIFIC EXPERIMENT] in Chinese No 10, Oct 79 pp 4-5

ABSTRACT: The mountains in Sichuan Province from X-chang to Dukou City is an area of wilderness, stretching 200 km. Chinese geologists and surveying workers have discovered a rich vanadium titano-magnetite reserve of tens of billion-tons. This is the Panzhihua ore deposit, a syngenetic production of more than 10 elements. The contents of vanadium, titanium, chromium, and cobalt are especially considerable. If all the iron content is made into superior quality steel, the value of which is regarded to be one, then, the value of the accompanying elements is 3-4 times greater. The difficulty involved in reclaiming these treasures is discussed. Many Chinese scientists have devoted themselves to the problem and have successfully created the technique of mist-blowing to reclaim vanadium from the slag. Aside from a brief description of the new technique, the paper also mentions continuous research and the promise of producing a third metal, following the black metal of iron-steel and the colored metal of molybdenum.

AUTHOR: LIU Renjun [0491 0088 0193]

ORG: None

TITLE: "Rare Treasure of the World--White Dolphin"

SOURCE: Beijing KEXUE SHIYAN [SCIENTIFIC EXPERIMENT] in Chinese No 10, Oct 79 pp 6-7

ABSTRACT: The giant panda as a rare animal of the world is already very famous, but the other rare animal, which is also existing only in China, is unknown to many people. This is the white dolphin. It is perhaps even more lovely if it can be tamed and kept in a zoo. The white dolphin belongs to the same order as whales, but it lives in the fresh water of the Yangzi only. The Yangzi globefish is its cousin. The cerebrum of the white dolphin is very well developed. The cerebrum of a white colphin of a body weight of 237 kg measures 525 cm^3 in volume and 590 g in weight. Its two hemispheres take turn to go to sleep. If this mechanism could be understood and learned by humans the time availabe for work and study,etc.may be greatly extended. A portrait of the largest white dolphin captured so far is reproduced in the paper.

AUTHOR: WANG Ding [3769 0002]

ORG: None

TITLE: "Notes on Animal Resources--The Beautiful and Rich Island of Taiwan"

SOURCE: Beijing KEXUE SHIYAN [SCIENTIFIC EXPERIMENT] in Chinese No 10, Oct 79 pp 8-9

ABSTRACT: The beautiful and rich island of Taiwan is the largest island of China, with a total area of 36,000 km^2. The summer is long and the climate is pleasant. The water of its Pacific coast may reach 3,000m in depth, but its eastern sea is a natural extension of the continental shelf along Fujian Province; the narrow channel is only 130 nautical miles in the narrowist part and the depth is no more than 100 m. Aside from a very brief description of fishes and birds, as well as marine mammals, which are specially abundant in the region of Taiwan, this paper also mentions the fact that Taiwan is also known as the "butterfly kingdom" of the world, with more than 400 species of butterflies flying in large quantities on the island all year long. Birds found on the island are also briefly mentioned.

AUTHOR: ZHAO Yi [6392 2496]
GUO Ren [6751 0088]

ORG: None

TITLE: "A Green World--A Tour of the Guangxi Botanical Garden"

SOURCE: Beijing KEXUE SHIYAN [SCIENTIFIC EXPERIMENT] in Chinese No 10, Oct 79 pp 9-10

ABSTRACT: The Guangxi Botanical Garden is less than half-an-hour's ride from Guilin City, in the famous scenic region of Yanshan Mountains. The authors, under the guidance of the retired chief of the garden, NI Xingren [0242 5281 0088] paid a visit. The chief led them to view the 4 rare plants, known as 4 treasures of Yanshan, including Ziwei [Lagerstroemia indica L. whose branches vibrate if it is lightly touched, Lyuemei [Prunus mume, S et Z.] whose branches and calyxes are green and the blosoms are white, Dangui [Osmanthus fragrans Lour] which is a cassia or cinnamon tree with red instead of white or yellow blosoms, and Hongdou [Abrus precatorius] which involves the legend of tyranny and romance. Aside from drawings of several rare species of the garden, the paper also mentions the books on the flora and medicinal herbs of Guangxi, which the research scientists of the garden have been writing and compiling.

AUTHOR: HUANG Wanbo [7806 8001 3134]

ORG: None

TITLE: "Investigations at Nihewan"

SOURCE: Beijing KEXUE SHIYAN [SCIENTIFIC EXPERIMENT] in Chinese No 10, Oct 79 pp 11-13

ABSTRACT: Nihewan is a village of several hundred families, located on the northern bank of Sangganhe River, in Yangyuan County, Hebei Province. It became famous in 1924, when an English scholar discovered many fresh water bivalve fossil oysters. In early June this year, the Chinese Quaternary Research Committee of the Third National Science Conference held a geological tour of Nihewan. Participants included related scientists from various areas of the country as well as foreign scientists from Western and Northern Europe and Australia. The group inspected the stratography, the plant and zoo fossils, and cultural relics of the stone age. The significance of this region for Quaternary geology, the discoveries of fossil mesohippus and fish fossils by the Institute of Vertebrate Paleontology and Paleoanthropology, Chinese Academy of Sciences in the 1970's, and other recent findings are briefly described.

AUTHOR: LIU Rushui [0491 1172 3055]

ORG: None

TITLE: "A New Member of the Ceramics Family--Infrared Ceramics"

SOURCE: Beijing KEXUE SHIYAN [SCIENTIFIC EXPERIMENT] in Chinese No 10, Oct 79 pp 14-15

ABSTRACT: Although ceramics has had a history of several thousand years, with the advance of science, the types and applications of ceramics are growing everyday. This paper introduces one of the newest members of the family of ceramics. It is a polycrystalline ceramic material capable of being penetrated by infrared radiation. The infrared sensitive organs of a rattlesnake, used by the blind rattlesnake for distinguishing food, stone, enemy, etc. are explained. The infrared guided missile and other military applications of infrared detectors are inspired by the rattlesnake. Many uses of this infrared ceramics are described. Manufacturers of infrared ceramics in China, if any, are not mentioned in the paper.

AUTHOR: CUI Jintai [1508 6855 3143]

ORG: None

TITLE: "A Flower Among Adhesives--an Inorganic Adhesive"

SOURCE: Beijing KEXUE SHIYAN [SCIENTIFIC EXPERIMENT] in Chinese No 10, Oct 79 pp 16-17

ABSTRACT: Most adhesives are made of either natural animal or plant glue or synthetic organic polymers. These can withstand temperatures of 60-220°C only. The inorganic adhesives, made primarily of silicate, borate, or phosphate form a new type of adhesives. Of these, the phosphate adhesive, made with a given ratio of copper oxide, can withstand a temperature above 1000°C. It can be used to glue ceramic or hard alloy blades and can virtually replace rivets, screws, welding, etc. to join just about everything. The paper begins with a story of using inorganic adhesive to repair a crack in a cylinder cover of the engine of a cargo ship loaded with steel materials on route to its destination in the Yangzi River.

AUTHOR: None

ORG: None

TITLE: "A Garden of New Sciences and Technology"

SOURCE: Beijing KEXUE SHIYAN [SCIENTIFIC EXPERIMENT] in Chinese No 10, Oct 79 pp 18-19

ABSTRACT: This paper contains 5 short items on the following: (1) Great progress in ore dressing experiment for red iron ores in China has been reported by several research institutes; experimental results for chalybit, hematite, and limonite demonstrate returns of 66-72 percent. (2)The 501 Group of the Institute of Genetics, Chinese Academy of Sciences has succeeded in obtaining seeds and progenies from vitro fertilization of corn oocytes. (3) Seven medical research organizations have reported studies on endophin, its extraction from human and rabbit brains, and its relationship with acupuncture analgesia. (4) A new type of L-W hydraulicking gun has been specially designed after an analysis of the major coal mines in China using hydraulic extraction. It has been certified as suitable for mining medium to thick layers of coal. (5) Electrical power quantity controller is designed for supplying power at a given time and in a given quantity. When it is installed, the power customer will hear an alarm when the power limit is reached and 15 minutes later the controller will switch off the supply of power.

AUTHOR: YU Shoucheng [0060 1343 6134]

ORG: None

TITLE: "Rocket Minelayer"

SOURCE: Beijing KEXUE SHIYAN [SCIENTIFIC EXPERIMENT] in Chinese No 10, Oct 79 pp 20-21, 48

ABSTRACT: According to related records, during WWII Germany lost ten thousand tanks and armored vehicles and several tens of thousands of men to various types of mines of the Soviet Union. In those days, it took about 5 hours to prepare a minefield of 1 km^2 in area. Today, with rocket minelayer, it takes less than one minute. Minelaying vehicle equipped with minelaying tubes for rocket minelaying is described. New types of minelayers being developed are briefly mentioned also. At the opening ceremoney of the Fourth all military athletic competition, rocket minelaying was demonstrated before an audience of several tens of thousands. The date and place of this performance are not mentioned.

AUTHOR: SHI Haoqun [2457 7729 5028]

ORG: None

TITLE: "Guided-Missile Submarine"

SOURCE: Beijing KEXUE SHIYAN [SCIENTIFIC EXPERIMENT] in Chinese No 10, Oct 79 pp 22-23

ABSTRACT: The modern submarine is a powerful weapon, capable of attacking coastal as well as ocean targets, but its major weapon, the torpedo, has many defects. Its trajectory is limited and it sometimes misses the target. After the guided missile made its appearance, it soon became the major weapon of submarines. A new type of submarine was designed to give it the additional capability of launching guided missiles. There are many types of guided missiles carried on submarines, including the strategic and the tacticle guided missiles; long, intermediate, and short distance guided missiles; the tube launched type and the flying type; the nuclear guided missile and the conventional guided missile; and the ship-targeted, the shore-targeted, the anti-submarine, and the air-defense guided missiles. There is a brief description of each of these types. New types of guided missiles being studied in the United States and the Soviet Union are briefly mentioned. There is no mention of Chinese guided missiles or submarines.

AUTHOR: ZHU Yilin [2612 3015 7792]

ORG: None

TITLE: "Space Station Attracts Everyone's Attention"

SOURCE: Beijing KEXUE SHIYAN [SCIENTIFIC EXPERIMENT] in Chinese No 10, Oct 79 pp 24-27

ABSTRACT: Ten years ago, the Apollo spacecraft successfully landed men on the moon and returned. Several hundred kg of moon rocks it brought back did not benefit mankind, however, and the enthusiasm about traveling to the moon diminished after awhile. In the 1970's, the attention has been on spaceships and space stations, in which men can live for prolonged periods of time to perform the tasks unable to perform by the machines of the unmanned satellites. This paper explains the functions of a space station, the manner and problems of men who live in a space station, etc. Finally, specifics of skylabs of the United States and the Soviet Union are given. The skylab of the U.S. launched in May 1973, had been left empty since Feb 74. After orbiting aimlessly for 5 years and 5 months, it crashed down on parts of Australia and the Indian Ocean. The Soviet Union did not relax its space program, however. The Salyut was launched in Sep 77 and its astronauts have been traveling back and forth 7 times. Many times, unmanned spacecrafts have supplied it with oxygen, food, and water; the latest trip was accomplished on 30 Jun this year.

AUTHOR: GU Yongkang [7357 3057 1660]
SHENG Guohua [4141 0948 5478]

ORG: None

TITLE: "Chorella Entered [Johnson Space Center in] Houston"

SOURCE: Beijing KEXUE SHIYAN [SCIENTIFIC EXPERIMENT] in Chinese No 10, Oct 79 pp 30-31

ABSTRACT: Chorella is a species of unicellular green algae. It is said that in primitive times,inhabitants of Japan dried it like salt to use it for food, but it tasted too much like grass to be popular. During WWI, there were attemps of processing it into food but nothing came out of them. Perhaps, its cell wall is too think to be readily digestible. It was not until the 1950's before its industrial refining became a success. It can propagate one hundred times in a day and the yield is 8 to 30 times of that of rice or soybean from a unit area. Some tonics being sold by foreign countries are in fact crystals of its extract. In 1957, a Chorella research institute was established in Japan. Several years ago, the U.S.A. began to use it in nuclear submarines to produce oxygen. A man's daily oxygen consumption, about 1500g can be supplied by 40 g of Chorella, while the carbon dioxide exhaled by the man is sufficient to supply the needs of the Chorella. Today, it has been reported that Chorella has been invited to Houston to become the food of astronauts.

AUTHOR: WANG Jianxun [3769 1696 8113]

ORG: None

TITLE: "New Techniques in the Realm of Medicine"

SOURCE: Beijing KEXUE SHIYAN [SCIENTIFIC EXPERIMENT] in Chinese No 10, Oct 79 pp 32-35

ABSTRACT: Many new techniques have been introduced to medicine in recent years to creat a great change in medical research and treatment. After computers are brought to the realm of medicine, a profound change has occurred to almost all traditional medical instruments. Today more than 300 electronic instruments are being used for diagnosis and treatment. Beside computers and electronics, the applications of laser technology, infrared radiation, ultrasonics, radioactive isotopes and rays, and high molecular materials are explained in separate headings in the paper.

AUTHOR: XIA Shan [1115 1472]

ORG: None

TITLE: "Mining Coal Under Three Places"

SOURCE: Beijing KEXUE SHIYAN [SCIENTIFIC EXPERIMENT] in Chinese No 10, Oct 79 pp 43-44

ABSTRACT: In some countries, coal, this food of industries, is everywhere. China is one of those. It is under the lakes and rivers; it is under the railroad tracks, and it is under our houses and buildings. For example, the entire city of Wushun is on top of millions of tons of superior quality coal capable of being refined into coke. In the early 1970's Poland succeeded in extracting coal safely from under cities and towns. Today, 40 percent of that country's coal production is mined under existing structures. Toward the end of 1960's, England succeeded in mining 7 percent of its total coal production from the sea bed. Experiments in these countries had proved that if reasonable mining procedures are adopted, the gound surface can be protected from sinking after the coal is removed. Problems and solutions of mining coal under a body of water, under railroad lines, and under buildings are explained.

AUTHOR: WU Peining [0702 1014 1337]

ORG: None

TITLE: "Giant Things in the Steel and Iron Industry"

SOURCE: Beijing KEXUE SHIYAN [SCIENTIFIC EXPERIMENT] in Chinese No 10, Oct 79 pp 45, 38

ABSTRACT: The tendency of the modern steel and iron industries is to have larger and larger plants, greater and greater production totals, and bigger and bigger tools. In the 1930's the average production per year of a joint steel and iron enterprise was 50 thousand to 1 million tons; it became 4-5 hundred million tons in the 60's and 8 hundred million to one billion tons today. The largest such enterprise is in Japan, having a yearly pproduction capacity of 1 billion 6 hundred million tons. These giant mills use giant tools. The drill has a downward pressure of 59 tons and the hole it produces measures 310-445 mm in diameter. The electrical shovel holds 19.1 m^3, the volume of 7 Chinese trucks; the giant truck has a load capacity of 350 tons; the open-hearth furnace refines 900 tons in one operation; the electrical furnace can hold 360 tons, the converter 400 tons, etc. The largest equipment of the various steel and iron industries of different countries of the world is briefly and separately described.

AUTHOR: (1) ZHANG Jiaqi [1728 0857 7871]

ORG: None

TITLE: "(1) Front Cover; (2) Inside Front Cover"

SOURCE: Beijing KEXUE SHIYAN [SCIENTIFIC EXPERIMENT] in Chinese No 10, Oct 79 front and inside front covers

ABSTRACT: (1) The front cover carries a photo, taken by the author, to depict the Panzhihua Iron Refining Mill. (2) The inside front cover contains a group of 4 photos concerning China's first high energy physics laboratory soon to be established in the vicinity of Beijing: (i) FANG Yi [2455 3015], Vice Premier and Director of Chinese Academy of Sciences carries out an on site inspection tour. (ii) Scientists and technicians discuss problems concerning the 50 billion electron volt synchronous accelerator in the process of being built. (iii) Scientists and technicians are adjusting the linear accelerator made by the Institute of High Energy Physics, Chinese Academy of Sciences. (4) The 250 kv pre-injector has been completely installed and is now being adjusted and tried.

6168
CSO: 4009

AN INVESTIGATION OF THE DIRECTIONAL SOLIDIFCATION OF A NICKEL-BASE SUPERALLOY

Shenyang JINSHU XUEBAO [ACTA METALLURGICA SINICA; METALLURGICAL JOURNAL] in Chinese Vol 15 No 2, Jun 79 p 186

Lin Dongliang [2651 2767 2733] and Yao Deliang [1290 1796 5328], Shanghai Jiaotong University

[Abstract] The structure and properties of a directionally solidified high strength cast nickel-base superalloy have been studied. Directional solidification significantly increased the resistance to thermal-fatigue and intermediate temperature rupture life as well as the ductility and the tensile strength and high temperature rupture life of the alloy. The improvement of rupture life at certain intermediate temperature (about 760°C) was found to be due to an extension of the secondary stage of creep, whereas at a high temperature (about 980°C) the same improvement came from an extension of the tertiary stage. The absence of grain boundaries in the transverse direction gave rise to better mechanical properties, in particular, the ‹100› preferred orientation of the columnar grains played an important part in the increased strength at elevated temperatures.

[continuation of JINSHU XUEBAO Vol 15 No 2, 2 Jun 79 p 186]

The secondary creep rate was lowered and the second creep stage extended after high temperature solution treatment. This was found to be due to the solutioning of the coarse γ' phase on heating and the subsequent reprecipitation of a uniformly dispersed fine γ' particles in the cast alloy after cooling.

In the above directionally solidified alloy, primary MC carbides seem to serve as the sites for creep and thermal-fatigue crack initiation. This rather suggests that the high temperature mechanical properties of the alloy may possibly be further improved if its carbon content is lowered.

CSO: 4020

EFFECT OF CERTAIN ALLOYING ELEMENTS ON THE MECHANICAL PROPERTIES OF A WROUGHT NICKEL-IRON BASE SUPERALLOY

Shenyang JINSHU XUEBAO [ACTA METALLURGICA SINICA; METALLURGICAL JOURNAL] in Chinese Vol 15 No 2, Jun 79 p 196

Wang Yunshi [3769 0336 1395]; Wang Sukun [3769 4790 0981]; Zhang Shunnan [Chinese characters not given], Institute of Metal Research, Academia Sinica; Zhao Yucai [6392 3768 2624], Shanghai No 5 Steel Works; and Li Shijin [2621 0013 0093], Shanghai Institute of Iron and Steel Research

[Abstract] The effects of certain alloying elements such as titanium, aluminum, molybdenum, carbon, boron, etc. on the tensile, impact and stress-rupture properties of a 42Ni-35Fe-13Cr superalloy have been investigated. Titanium or molybdenum increased the 0.2% proof stress, the elongation, and the impact properties at room temperature as well as the stress-rupture life of the alloy at elevated temperatures. The presence of aluminum up to 0.3% accelerated the formation of γ'-Ni_3 (Ti, Al). Carbon and boron promoted the formation of fine grain size, with an optimum at 0.035% C and 0.010% B, where a maximum stress-rupture life of such an alloy was obtained. The strengthening mechanism of the above alloying elements and their optimum contents are discussed. It is emphasized that a close control of the carbon and boron contents of the alloy and demand of high quality and cleanness of the ingot are particularly important.

CSO: 4020

AN INVESTIGATION OF QUASI-CLEAVAGE FRACTURE IN STEEL

Shenyang JINSHU XUEBAO [ACTA METALLURGICA SINICA; METALLURGICAL JOURNAL] in Chinese Vol 15 No 2, Jun 79 p 265

Liao Qian [1675 0051 0443], Sun Fuyu [1327 4395 3768] and Lan Fenlan [5663 5358 5695], Beijing Institute of Iron and Steel Research

[Abstract] The quasi-cleavage fracture has been studied in conjunction with the stress strain behaviour of steel specimens. Consideration of the results obtained on different varieties of steel indicate that the quasi-cleavage fracture may be interpreted in terms of certain transition fracture as follows:

Microcleavage cracks are nucleated at certain places of high tensile stress concentration, subsequently each of them propagates along the cleavage plane in grains already deformed and finally they merge together by microplastic coalescence. According to the above conception, the interaction between the cleavage crack and the plastic deformation may be regarded as the most important characteristics of quasi-cleavage fractures. Using quantitative fractography, correlation between the fractographic features of specimens and the parameters of its certain mechanical properties may be established.

CSO: 4020

APPLICATION OF ETCH-FIGURE METHOD FOR THE EXAMINATION OF SILICON-IRON

Shenyang JINSHU XUEBAO [ACTA METALLURGICA SINICA; METALLURGICAL JOURNAL] in Chinese Vol 15 No 2, Jun 79 p 251

Luo Yang [5012 7122] and Lu Qichun [0712 0366 2504], Beijing Institute of Iron and Steel Research

[Abstract] Certain improvements of the etch-figure method, suitable for such fine-grained specimens as the matrix of primary recrystallization of the non-oriented silicon iron, are described. The determination of the geometrical parameters of the etch-figures by conventional metallographic microscope is also given. The usefulness of the etch-figure method is supported by many practical examples, e.g. determining the misorientation between the neighbouring grains, measuring the orientation and the textures, analysing the fractures, examining the orientation effect of domain structures, ascertaining the deformation extent of deformed grains as well as indicating the orientation relationships between the precipitants and its matrix, etc. Scanning electron microscope is very helpful for detailed observation and exact measurements of the etch pits, because of its long depth of view.

CSO: 4020

AN INVESTIGATION OF MAGNETIC Ni-Fe-Mo AND Ni-Fe-Nb ALLOYS

Shenyang JINSHU XUEBAO [ACTA METALLURGICA SINICA; METALLURGICAL JOURNAL] in Chinese Vol 15 No 2, Jun 79 p 258

Xu Wenchong [1776 3306 1504], Wang Junjian [3769 0193 0256], Su Xiujin [5685 4836 6930] and Li Zhihua [2621 1807 5478], Beijing Institute of Iron and Steel Research

[Abstract] An investigation of the structures of Ni-Fe-Mo and Ni-Fe-Nb alloys has been carried out by means of TEM supplemented by electron diffraction and X-ray diffraction analysis. The results obtained have been correlated with magnetic properties as follows:

Both alloys showed modulated structures, in which the Ni-Fe-Nb alloy being coarser and more predominant. As the proportion of modulated structures increases, the hardness of the alloy also increases, but vice versa in the case of its magnetic permeability.

[continuation of JINSHU XUEBAO Vol 15 No 2, Jun 79 p 258]

The introduction of ...ute atoms Mo and Nb would lower the degree of ordering in Ni_3Fe alloy, but fortunately only certain degree of ordering was sufficient to yield conditions for high permeability. A precipitating phase possessing the fcc (ordered) Ni_3Nb (γ'') structure and being coherent with the matrix, was observed in the Ni-Fe-Nb alloy. This phase appears to promote the formation of modulated structures and exert a strengthening effect on matrix.

CSO: 4020

THE EFFECT OF η-PHASE IN AN IRON-NICKEL-BASE SUPERALLOY

Shenyang JINSHU XUEBAO [ACTA METALLURGICA SINICA; METALLURGICAL JOURNAL] in Chinese Vol 15 No 2, Jun 79 p 202

Ge Yunlong [5514 0061 1803] Zhang Yongchang [7893 3057 2490] and Hou Cuiping [0186 5050 5493], Institute of Metal Research, Academia Sinica

[Abstract] The γ'-η transformation and the formation of the η-phase itself on the mechanical properties and hot-workability of an iron-nickel base superalloy (Fe-42Ni-13Cr-6Mo-2.8Ti-0.3A) has been studied. The formation of η-phase was promoted by increment of titanium content as well as by hot-working energy, and was retarded by the addition of aluminum, molybdenum and minute boron. When such an alloy did contain certain amount of η-phase, its rupture strength and/or stress-rupture life were reduced although its ductility and hot-workability were increased.

CSO: 4020

AN INVESTIGATION OF THE OXIDATION AND HOT CORROSION OF A 35Ni-15Cr TYPE IRON-BASE ALLOY

Shenyang JINSHU XUEBAO [ACTA METALLURGICA SINICA; METALLURGICAL JOURNAL] in Chinese Vol 15 No 2, Jun 79 p 214

Guo Jianting [6753 1696 0080], Institute of Metal Research, Academia Sinica

[Abstract] The oxidation behavior of a 35Ni-15Cr type iron-base superalloy in air over the temperature range of 700 to 1000°C for period up to 200 hours has been studied. The results obeyed the conventional parabolic law from which the values of activation energy Q_{p1} = 41 and Q_{p2} = 46 kcal per mole were estimated. The diffusion of Cr ions in Cr_2O_3 was obviously the governing factor to oxidation rate and X-ray analysis indicated that the surface scale consisted mainly of Cr_2O_3 with a certain amount of $(Cr,Fe)_2O_3$, TiO_2 and $NiCr_2O_4$. The results were confirmed by electron probe, showing surface enrichment of Cr, Fe and Ti. The scale was dense and tightly adhered to the surface of the oxidized specimen. If such an alloy was previously alumited, its oxidation-resisting and anti-corrosion properties were markedly improved and the scale, being enriched with Al, Cr and Ti, now consisted mainly of

[continuation of JINSHU XUEBAO Vol 15 No 2, Jun 79 p 214]

a-Al_2O_3 with minute $Fe(Cr,Al)_2O_4$ and TiO_2. With alumiting, the scale was more dense and more tightly adhered to surface than without alumiting.

CSO: 4202

THE BEHAVIOUR OF ALLOYING ELEMENTS IN MARINE LOW-ALLOY STEELS, II. THE INFLUENCE OF ALLOYING ELEMENTS ON THE LOCALISED CORROSION PROPERTY OF LOW-ALLOY STEELS IN ARTIFICIAL SEAWATER

Shenyang JINSHU XUEBAO [ACTA METALLURGICA SINICA; METALLURGICAL JOURNAL] in Chinese Vol 15 No 2, Jun 79 p 234

Joint Research Group of Corrosion, Shanghai Institute of Iron and Steel Research & Changchun Institute of Applied Chemistry, Academia Sinica

[Abstract] The effect of the alloying elements on localised corrosion properties of low-alloy steels has been studied by simulation of an occluded anode cell. Si or Al showed very strong beneficial main-effect, and at the same time often exerted important influence on the behaviour of other elements. In the latter respect, Si was the stronger of the two. The beneficial effect of Cr was marked when the Si content was low (0.1-0.2%), and completely disappeared when Si was increased to 0.8-1.0%. Cu behaved somewhat opposite to that of Cr. Mo promoted the beneficial effect of Si or Cr, although the main effect of itself alone was unbeneficial. The main effect of Ni is weak, however, it could match with Cu, Mo and Cr-Al to yield beneficial results. With regard to the two elements which were present in steel only in small amount, V was preferable to Nb.

CSO: 4020

QUANTITATIVE PHASE ANALYSIS BY X-RAY WITHOUT ANY STANDARD IN TEXTURED MATERIALS

Shenyang JINSHU XUEBAO [ACTA METALLURGICA SINICA; METALLURGICAL JOURNAL] in Chinse Vol 15 No 2, Jun 79 p 273

Lin Shuzhi [2651 2885 2535], Institute of Metal Research, Academia Sinica

[Abstract] Formulae derived for X-ray quantitative phase analysis without any standard in the case of specimens with identical texture have been shown to be in complete agreement with those derived by Zevin for randomly oriented specimens. Thus, when it is practicable by some ways (for example, by certain heat treatments) to change the composition of the alloy phases without altering the texture of the specimen, the method of quantitative phase analysis for such a textured specimen can be taken as identical with that for randomly oriented specimens.

In cases where the absorption coefficients of the phases in a specimen happen to be large, corrections for microabsorption are necessary and such corrections are given in the present work.

[continuation of JINSHU XUEBAO Vol 15 No 2, Jun 79 p 273]

The method mentioned above has been applied to a cold-rolled Fe-25%Mn alloy as well as to certain compacting specimens of Mo-Cu powders with satisfactory results.

CSO: 4020

'SINGLE GRAIN' OSCILLATING CRYSTAL METHOD FOR ULTRAMICROANALYSIS BY X-RAY

Shenyang JINSHU XUEBAO [ACTA METALLURGICA SINICA; METALLURGICAL JOURNAL] in Chinese Vol 15 No 2, Jun 79 p 282

Wu Qixing [0702 1142 2502] and Qin Daoxiang [6009 6670 3276], Research Institute of Daye Steel Works

[Abstract] X-ray identification of certain superfine grains weighing 0.003 μg each has been carried out by means of "single grain" oscillating crystal method in an ordinary Debye-Scherrer camera. The principle of this method, the measurement and the calculation of the diffraction angles, the number of diffraction spots and their relative intensities in reference to the relevant ASTM cards are discussed in detail. Attempts have also been made to revealing the presence of certain rare earth inclusions by this method as well as to further verifying the proposed formula.

CSO: 4020

DETECTION OF THE INITIATION OF CRACK BY A.C. POTENTIAL METHOD

Shenyang JINSHU XUEBAO [ACTA METALLURGICA SINICA; METALLURGICAL JOURNAL] in Chinese Vol 15 No 2, Jun 79 p 291

Research Group of Fracture Toughness, Institute of General Machinery Research

[Abstract] The principle and characteristics of the A.C. potential method for crack detection has been described. Various types of steel specimens including ferritic, ferrite-pearlitic, martensitic or austenite etc. have been examined by this method. Attempts have been made to clarify the different patterns of potential curves associated with the different steels, the relation between the peak values of potential curves and the initiation of cracking, and the relation between the increment of potential and the crack growth. Factors causing changes on the potential curves are tentatively discussed.

CSO: 4020 END

SELECTIVE LIST OF JPRS SERIAL REPORTS

CHINA SERIAL REPORTS

CHINA REPORT: Agriculture
CHINA REPORT: Economic Affairs
CHINA REPORT: Plant and Installation Data
CHINA REPORT: Political, Sociological and Military Affairs
CHINA REPORT: RED FLAG*
CHINA REPORT: Science and Technology

WORLDWIDE SERIAL REPORTS

WORLDWIDE REPORT: Environmental Quality
WORLDWIDE REPORT: Epidemiology
WORLDWIDE REPORT: Law of the Sea
WORLDWIDE REPORT: Nuclear Development and Proliferation
WORLDWIDE REPORT: Telecommunications Policy, Research and Development

*Cover-to-cover

END OF FICHE

DATE FILMED

7 May '80

MAK